BNL-224546-2023-TECH

EIC-ADD-TN-057

On polarization and snake arrangements in RHIC: Case of RHIC and EIC HSR tunes p and 3He

F. Méot

May 2023

Electron-Ion Collider

Brookhaven National Laboratory

U.S. Department of Energy

USDOE Office of Science (SC), Nuclear Physics (NP) (SC-26)

DISCLAIMER

EIC TECHNICAL NOTE	NUMBER EIC-ADD-TN-057
AUTHOR **François Méot**	DATE May 15, 2023

On polarization and snake arrangements in RHIC
Case of RHIC and EIC HSR tunes
p and 3He

Abstract

This Tech. Note summarizes the outcomes of numerical simulations of strong resonance crossing using RHIC lattice, as a tentative assessment of HSR expectations, with variants including: regular RHIC tunes, HSR fractional tune values, collision or injection optics, and various 2, 4 or 6 snake configurations. This is a first part of simulation studies regarding RHIC and the EIC HSR lattices, a second part concerns the latter specifically and will be released in a separate Tech Note.

Contents

1 Introduction

This Tech. Note summarizes the outcomes of numerical simulations of strong resonance crossing using RHIC lattice, collision optics. Various snake configurations are addressed,

(i) 2 snakes at the regular 3 o'clock and 9 o'clock locations,

(ii) 6 snakes all $\pi/3$ distant,

(iii) 4 snakes.

In Case (i), two different working points are tracked, nominal RHIC Qx/Qy=28.685/29.673 in some detail, and, briefly, EIC HSR fractional tunes, namely Qx/Qy=28.228/29.21.

Case (i) in addition is tracked with a few points of particular interest in mind:

- 15% of polarization are lost between 100 GeV and 255 GeV at RHIC, simulations may reveal possible cause(s),

- compared to RHIC, EIC HSR features a loss of 3-periodicity, which is expected to cause greater excitation of systematic resonances: comparing simulation outcomes may help clarifying this point,

- whether the integer part of ν_y matters. Note that changing the integer part of RHIC tunes affects the optics in a substantial manner, the case is left for future reporting.

2 Conclusion: Recap Table

Table 1 summarizes the outcomes of the numerical simulations detailed in Appendix.

Table 1: A summary of crossing simulation outcomes. Unless otherwise specified, regular RHIC tunes are used, Qx/Qy=28.685/29.673. Unless otherwise specified, $\dot{\gamma} = 1$.

		rms orbit defect (mm)	Polarization loss	Refer to
proton, 2 snakes				
Regular RHIC tunes				
$\epsilon_x/\pi = \epsilon_y/\pi = 2.5\,\mu$m	393+Qy	none	$< 1\%$	Fig. 8
		0.6	$< 1\%$	Fig. 10
	245-Qy & 255-Qy	none	$< 1\%$	Fig. 11
$\epsilon_x/\pi = \epsilon_y/\pi = 1\,\mu$m	393+Qy	none	$< 1\%$	Fig. 14
		0.6	$< 1\%$	Fig. 16
$\epsilon_x/\pi = 2\,\mu$m, $\epsilon_y/\pi = 0.5\,\mu$m	393+Qy	none	$< 1\%$	Fig. 19
		0.3	$< 1\%$	Fig. 21
		0.6	$< 1\%$	Fig. 22
HSR fractional tunes, $\epsilon_x/\pi = \epsilon_y/\pi = 2.5\,\mu$m				
Qx/Qy=28.228/29.210	393+Qy	none	$\approx 20\%$	Fig. 23
Qx/Qy=28.228/29.170	393+Qy	none	$\approx 20\%$	Fig. 24
Qx/Qy=28.228/29.210	411-Qy	none	$\approx 10\%$	Fig. 25
Qx/Qy=28.228/29.190	411-Qy	none	$\approx 2\%$	Fig. 26
3He, 2 snakes				
$\dot{\gamma} = 6$				
$\epsilon_x/\pi = \epsilon_y/\pi = 2.5\,\mu$m	735-ν_y	none	strong	Fig. 29
	717+ν_y	none	strong	Fig. 29
$\epsilon_x/\pi = \epsilon_y/\pi = 1\,\mu$m	735-ν_y	none	strong	Fig. 30
	717+ν_y	none	strong	Fig. 30
$\epsilon_x/\pi = 2\,\mu$m, $\epsilon_y/\pi = 0.5\,\mu$m	735-ν_y	none	$< 1\%$ [(a)]	Fig. 31
	717+ν_y	none	$\approx$percent(s)	Fig. 31
3He, 6 snakes				
$\epsilon_x/\pi = \epsilon_y/\pi = 2.5\,\mu$m, $\dot{\gamma} \geq 6$	735-ν_y	none	$\approx$percent(s)	Figs. 35, 37
$\epsilon_x/\pi = \epsilon_y/\pi = 1\,\mu$m, , $\dot{\gamma} = 6$	735-ν_y	none	$< 1\%$ [(b)]	Fig. 39
	717+ν_y	none	none [(b)]	Fig. 39
$\epsilon_x/\pi = 2\,\mu$m, $\epsilon_y/\pi = 0.5\,\mu$m, $\dot{\gamma} \geq 1$	717+ν_y	none	none	Fig. 41
		0.6	none	Fig. 42
3He, various 4 snake arrangements				
$\epsilon_x/\pi = \epsilon_y/\pi = 2.5\,\mu$m, $\dot{\gamma} = 2$	717+ν_y	none	$> 20\,\%$	Figs. 43, 44
	717+ν_y	0.6	100 %	Fig. 44
$\epsilon_x/\pi = 2\,\mu$m, $\epsilon_y/\pi = 0.5\,\mu$m, $\dot{\gamma} \geq 2$	717+ν_y	none	none [(b)]	Figs. 45, 46
	717+ν_y	0.6	100 %	Fig. 46

(a) Could be worth checking with $\dot{\gamma} = 1$ instead; however 717+ν_y losses are prohibitive.
(b) To be confirmed with $\dot{\gamma} = 1$ instead.

It can be drawn from these results that, simulation-wise,

- Proton, 2 snakes, $2.5\,\pi\mu$m emittances:
  - the crossing of 393+Qy with regular RHIC tunes Qx/Qy=28.685/29.673, and including 0.6 mm *rms* vertical closed orbit, shows marginal depolarization.
  - instead, with EIC HSR tunes, namely Qx/Qy=28.228/29.210, both 393+Qy and 411-Qy crossings result in substantial depolarization. Mitigated if frac(Qy) decreased away from 0.21.

- 3He, 2 snakes, vertical emittance down to $0.5\,\pi\mu$m:
  - does not preserve polarization
- 3He, 6 snakes:
  - polarization not preserved if vertical emittance $\geq 1\,\pi\mu$m
  - indications that polarization is preserved in the presence of 0.6 mm vertical closed orbit, if $\epsilon_y/\pi = 0.5\mu$m.
- 3He, various 4 snake arrangements:
  - vertical emittance $\epsilon_y/\pi = 2.5$ or $1\ \mu$m: polarization is lost
  - $\epsilon_y/\pi = 0.5\mu$m:
    - polarization is preserved in the absence of orbit defect
    - polarization loss (or fully lost) in the presence of vertical closed orbit.

Appendix

A RHIC Lattice Model

Possible polarization loss upon crossing the strongest intrinsic resonance $G\gamma = 393 + \nu_y \sim 423$, near the end of the ramp to store energy, is investigated. This is close to RHIC 255 GeV ($G\gamma \sim 487$) store energy, thus RHIC lattice store optics is assumed in these simulations, Fig. 1.

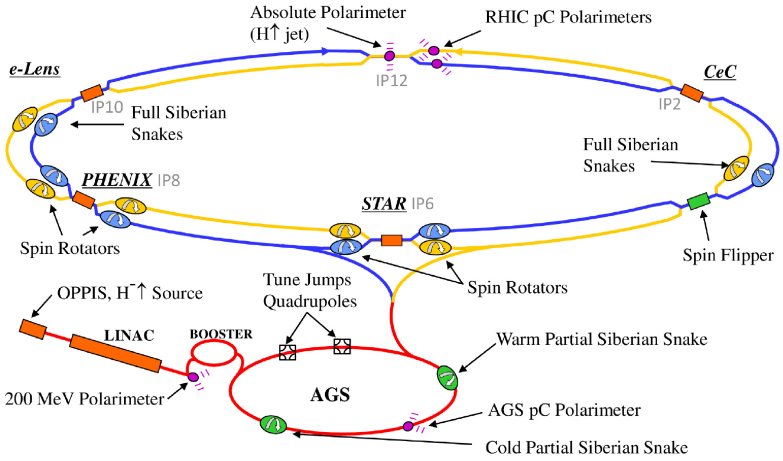

A.1 Optics

In the following tracking simulations, the same lattice is used for both RHIC working point settings, Qx/Qy=28.685/29.673 and Qx/Qy=28.228/29.210.

The same lattice as well is used for p and 3He, with working point Qx/Qy=28.685/29.673.

A.1.1 Nominal RHIC tunes, Qx/Qy=28.685/29.673

Optical data are detailed in Tab. 2.

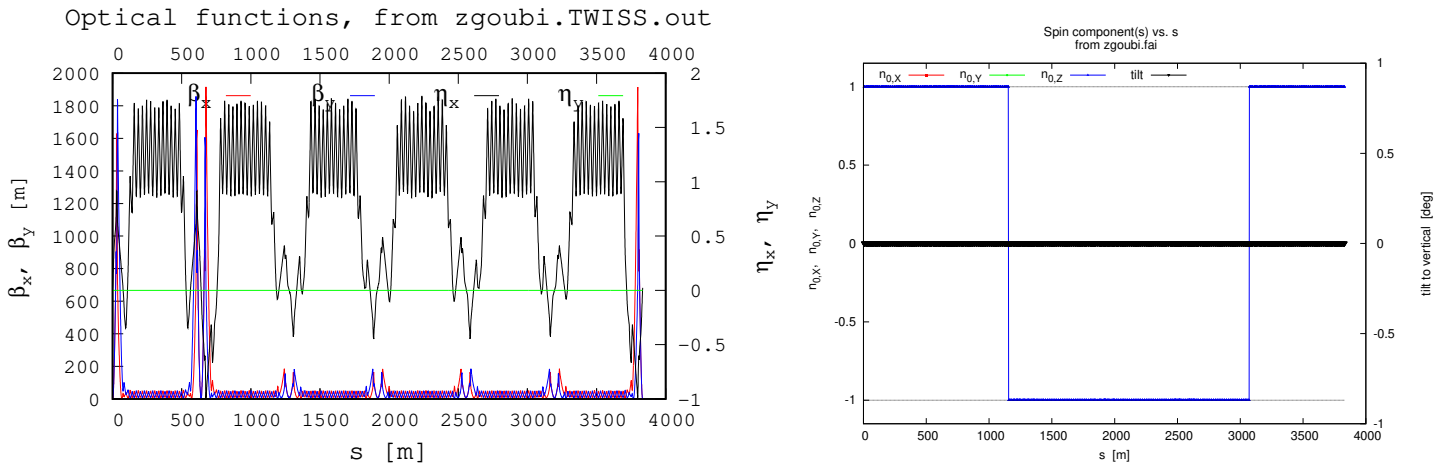

Figure 1: Lattice used for polarization tracking, case Qx/Qy=28.685/29.673. optical functions, left, and, right: stable spin precession direction components and its tilt angle to vertical (Z-axis).

Table 2: Optical parameters of the lattice used for polarization tracking in the case Qx/Qy=28.685/29.673.

@ LENGTH	3833.846023		
@ ALFA	0.1779389801E-02		
@ Q1	**28.6850251018**		
@ Q2	**29.6730125830**		
@ DQ1	0.5950638457		
@ DQ2	1.344023907		
@ DXMAX	1.78659079E+00	@ DXMIN	-9.89909831E-01
@ DYMAX	0.00000000E+00	@ DYMIN	0.00000000E+00
@ XCOMAX	6.48256441E-05	@ XCOMIN	-6.26719419E-07
@ YCOMAX	0.00000000E+00	@ YCOMIN	0.00000000E+00
@ BETXMAX	1.91591785E+03	@ BETXMIN	7.09100207E-01
@ BETYMAX	1.85831207E+03	@ BETYMIN	6.95108249E-01
@ XCORMS	2.13654342E-07		
@ YCORMS	0.		
@ DXRMS	7.00053138E-01		

A.1.2 Case of HSR fractional tunes, Qx/Qy=28.228/29.21

Case of RHIC lattice with HSR fractional tunes. Optical data are detailed in Tab. 3.

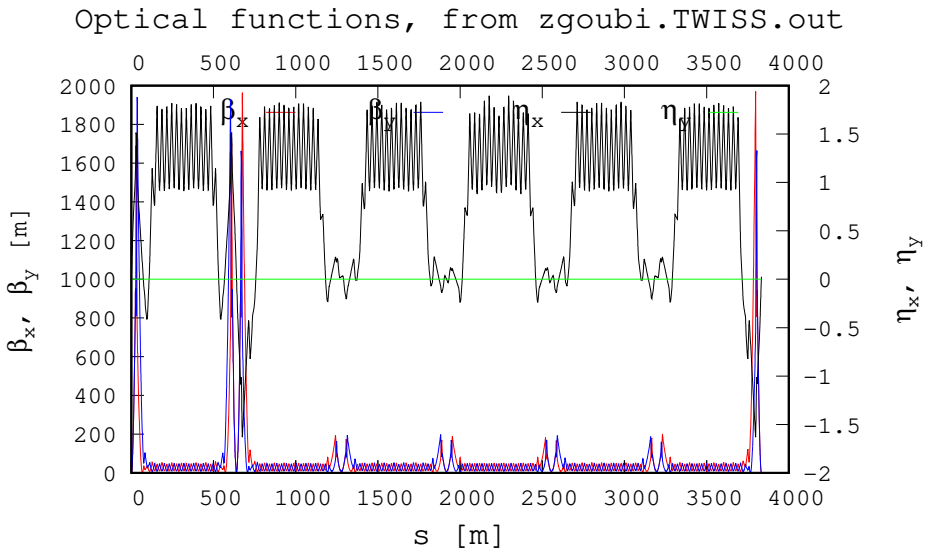

Figure 2: Lattice used for polarization tracking, case of HSR fractional tunes: Qx/Qy=28.228/29.21.

Table 3: Optical parameters of the lattice used for polarization tracking in the case Qx/Qy=28.228/29.21.

@ LENGTH	3833.846023		
@ ALFA	0.1867923676E-02		
@ ORBIT5	-0		
@ GAMMATR	23.13771336		
@ Q1	**0.22800939E+00 28 [frac., int.]**		
@ Q2	**0.21000347E+00 29 [frac., int.]**		
@ DQ1	1.778537026		
@ DQ2	1.123495542		
@ DXMAX	1.89269985E+00	-1.63091073E+00	@ DXMAX/MIN
@ DYMAX	0.00000000E+00	0.00000000E+00	@ DYMAX/MIN
@ XCOMAX	2.06836738E-04	-7.70497520E-07	@ XCOMAX/MIN
@ YCOMAX	0.00000000E+00	0.00000000E+00	@ YCOMAX/MIN
@ BETXMAX	1.96986157E+03	7.04694703E-01	@ BETXMAX/MIN
@ BETYMAX	1.94079093E+03	6.78608835E-01	@ BETYMAX/MIN
@ XCORMS	3.20792568E-07		
@ YCORMS	0.		
@ DXRMS	7.80531305E-01		

A.2 Resonance Strengths

Strengths ϵ_n of resonances at $G\gamma = \text{integer} \pm \nu_y$ are calculated for $\epsilon_{\mathbf{y}} = \mathbf{10}\pi\mu$m, using [2]

$$\left\{ \begin{array}{c} \mathcal{R}e(\epsilon_n^{\text{intr},\pm}) \\ \mathcal{I}m(\epsilon_n^{\text{intr},\pm}) \end{array} \right\} = \frac{1+G\gamma_n}{4\pi} \sum_{\text{Qpoles}} \left\{ \begin{array}{c} \cos(G\gamma_n\alpha_i \pm \varphi_i) \\ \sin(G\gamma_n\alpha_i \pm \varphi_i) \end{array} \right\} (KL)_i \sqrt{\beta_{y,i}\frac{\varepsilon_y}{\pi}} \tag{1}$$

The envelop equation [3, Eq. 5.37]

$$< S_y >= 1 - 8a^2(1-a^2), \quad a = \frac{|\epsilon_K|}{\lambda} \sin\frac{\pi\lambda}{2}, \quad \lambda = ((G\gamma - G\gamma_{\text{res.}})^2 + |\epsilon_K^2|)^{1/2} \tag{2}$$

is used for occasional checks of resonance crossing outcomes.

A.2.1 Nominal RHIC tunes, Qx/Qy=28.685/29.673

Resonance strengths with collision optics (Fig. 1) are displayed in Fig. 3-left (proton) and Fig. 3-right (3He).

In these simulations collision optics has also been used for resonance crossing in the $\gamma \sim 100 - 150$ region, for simplicity. It does not preclude re-doing it with actual settings (or injection settings) ... Anyway, this leaned on the observation, Figure 5, that resonance structure and strengths with injection optics does not differ much from collision optics case, in particular non-systematic resonances have similar strengths as well, in spite of a breaking of 3-periodicity with collision optics due to β^* squeeze at IP6 and IP8 (Fig. 2).

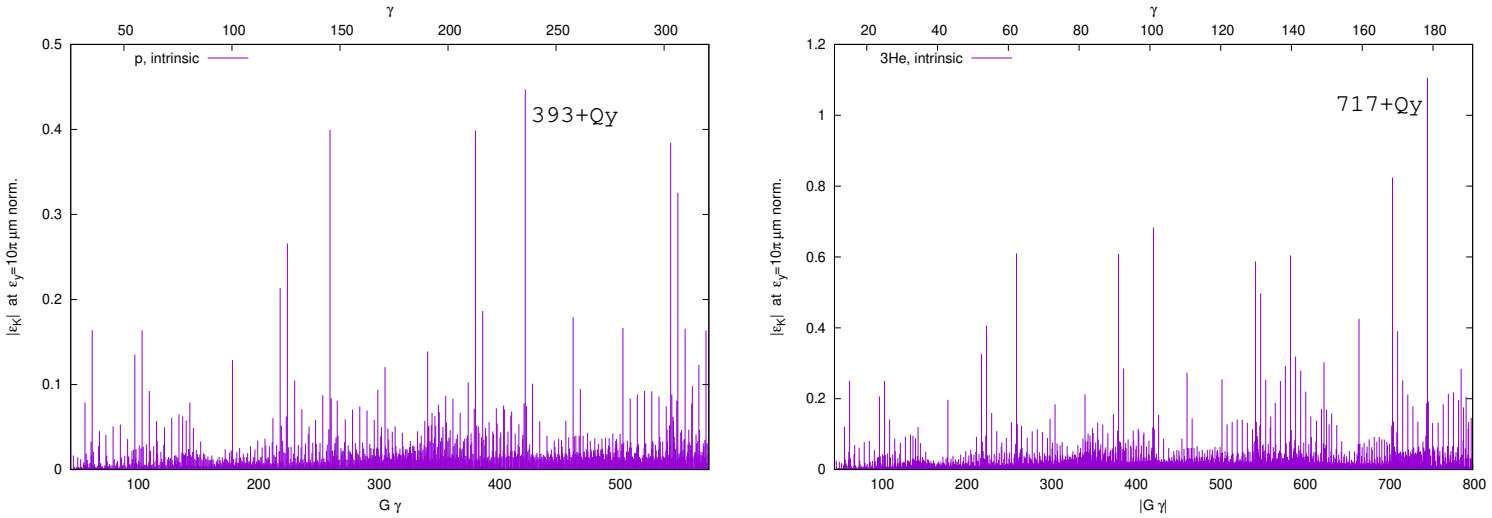

Figure 3: Strength of intrinsic resonances, collision optics, case $\epsilon_y = 10\pi\mu$m, normalized. RHIC is set to $\nu_y = 29.6730$. Proton, left graph: the strongest resonance upstream of the 275 GeV EIC as well as RHIC 255 GeV top energy is at $G\gamma = 393 + \nu_y$, $\epsilon_K = 0.447154$. Helion, right graph: the strongest resonance upstream of the 170 GeV EIC top energy is at $|G\gamma| = 717 + \nu_y$, $\epsilon_K = 1.1059$

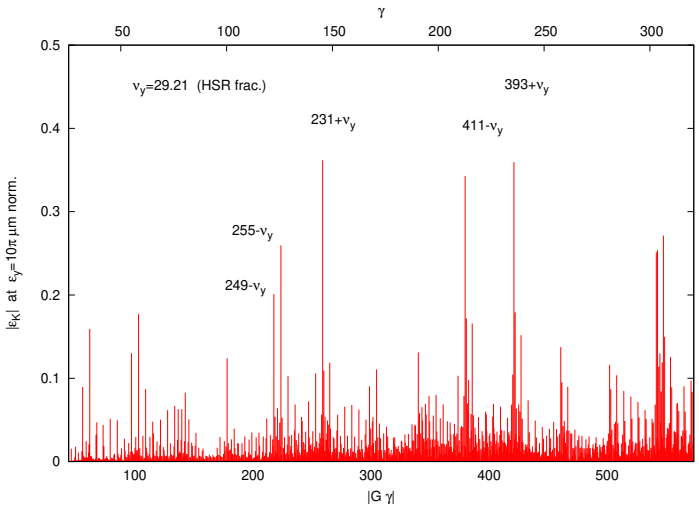

Figure 4: Strength of intrinsic resonances, proton, injection optics ($\beta_{\max} \approx 150$), nominal RHIC tunes Qx/Qy=28.685/29.673.

A.2.2 Case of EIC HSR fractional tunes, Qx/Qy=28.228/29.21

Case of RHIC lattice with HSR fractional tunes. No dramatic difference in resonance strengths (Fig. 5), compared to nominal tunes Qx/Qy=28.685/29.673, which is expected as the two optics are quite similar (Sects. A.1.1, A.1.2). The numerology of the resonances changes by ± 1 unit of $G\gamma$.

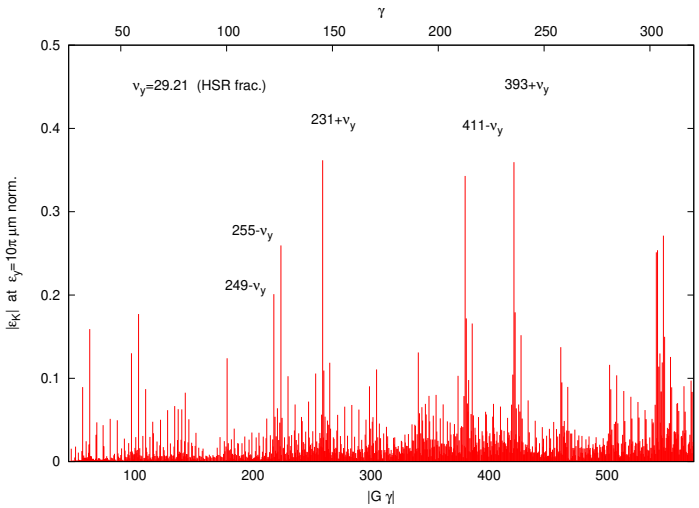

Figure 5: Strength of intrinsic resonances, proton, $\epsilon_y = 10\pi\mu$m, normalized, collision optics, with $\nu_y = 29.21$ (optical functions appear to be very similar to the case of nominal tunes of Fig. 2).

A.3 RF settings

They are the same for both species, namely:

```
'CAVITE'  accelerating cavity
2                                   ! option: Synchrotron cavity
3833.84593000000    360.00          ! closed orbit length; harmonic number
300e3     2.792526803191            ! peak voltage (V), synchronous phase (rad)
```

Zgoubi data:

```
 6769  Keyword, label(s) :  CAVITE      accelerating

 Orbit  length                =   3.83384593E+03 m
 RF  harmonic h               =   3.60000000E+02
 Peak  voltage                =   3.50000000E+04 V
 f_rev * h                    =   2.81496253E+07 Hz
 Synchronous  phase           =   2.79252680E+00 rd
 Isochronous  time            =   1.27888026E-05 s
 particle charge (Q/QE)       =   1.00000000E+00
 Q*V*sin(phi_s)               =   1.19707050E-02 MeV
 cos(phi_s)                   =  -9.39692621E-01
 dp-acc*sqrt(alpha)           =   1.71705635E-05
 dgamma/dt                    =   9.97647186E-01 /s
 rho*dB/dt                    =   3.12237509E+00 T.m/s
 SR loss, this pass           =   0.00000000E+00 MeV
 Cavity azimuth        s      =   3.83384603E+05 m
```

Actual operation uses peak RF voltage of, e.g. in Run 22, 33 kV to 35 kV, for instance $B\rho$-dot=2 in Yellow, 4 in Blue, picture above.

$\hat{V}$ is taken 35 kV in most trackings, for gamma-dot=1, proton, or greater for faster simulation.

However, in the simulations performed so far it is observed that polarization transmission with snakes through RHIC strong intrinsic resonances is essentially independent of crossing speed. This seems consistent with $\frac{7}{10}$-th resonance crossing measurements at RHIC reported in

https://accelconf.web.cern.ch/p07/PAPERS/TUPAS086.PDF.

From the RF settings above, it results for protons (q=1)
- 35 kV peak-V yields $\dot{\gamma} = 1\, s^{-1}$.
- At 300kVolts*q*sin(2.7925268) = 102 kV/turn, $\dot{\gamma} = 8.55\, s^{-1}$. This is about 7 times RHIC Run 22 proton operation $\dot{\gamma} = 1.237\, s^{-1}$ (after RHIC elogs - pic on the right, where 393+ resonance crossing appears still at maximum $B\rho$-dot)

For helion, the acceleration rate is twice as much (q=2).

B Proton, 2 snakes

B.1 Case of nominal RHIC tunes, Qx/Qy=28.685/29.673

B.1.1 Transverse emittances $\epsilon_x/\pi = \epsilon_y/\pi = 2.5\ \mu$m, for reference

$\epsilon_x/\pi = \epsilon_y/\pi = 2.5\ \mu$m are typical RHIC polarized proton run emittance values. This case is tracked for reference, to permit comparison with different emittance cases in the next Sections.

• Initial phase-spaces

(x,x'), MATCHED (y,y'), MATCHED (dl, dp/p), NOT MATCHED

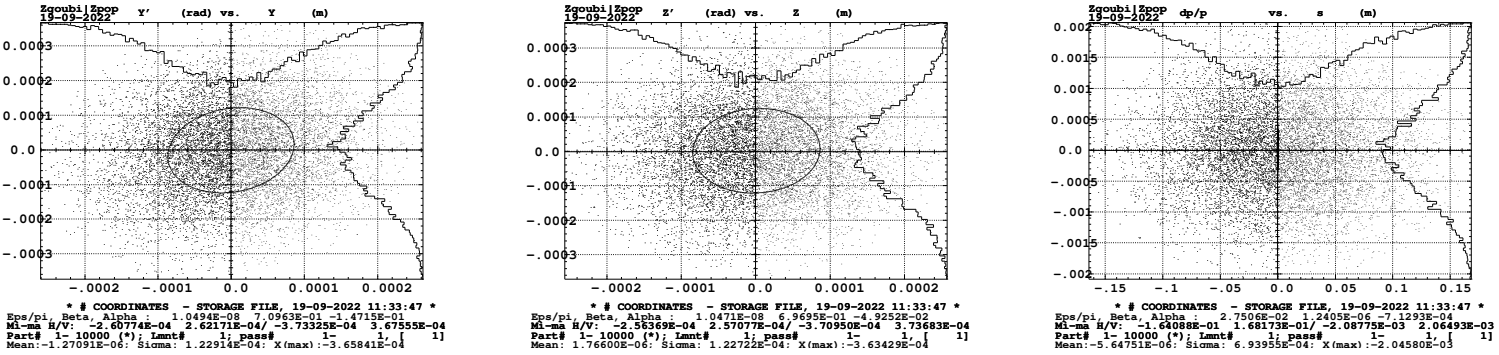

Figure 6: Initial phase spaces, at IP6, matched to lattice: horizontal, vertical, longitudinal (l-dp).

Multi-turn monitoring:

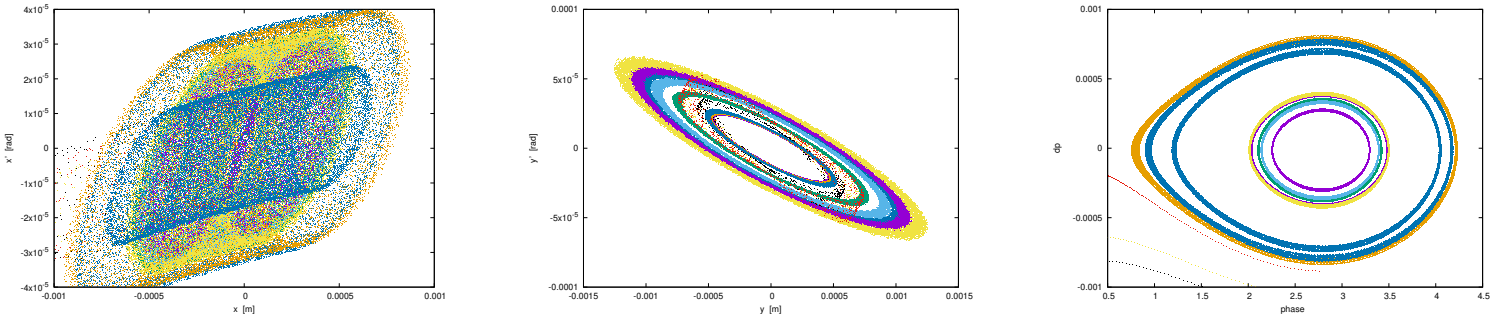

Figure 7: Monitoring: 185,000-turn phase spaces, a few particles (different colors), observation is at 9 o'clock snake. Incidentally, a particle is beyond momentum acceptance here.

Spin matrix at IP6:

```
 Sanity check:  spin transfer matrix, momentum group # 1 :

      -1.00000        6.158643E-06   -3.528648E-18
     -6.158643E-06     -1.00000       -2.223735E-16
     -3.530017E-18   -2.223735E-16      1.00000

Determinant =     1.0000000000
Trace =    -1.0000000000;  spin precession acos((trace-1)/2) =   179.9996471363 deg
```

Precession axis : (0.000000, 0.000000,-1.000000) -> angle to vertical is 180.0000 deg

Spin precession/2pi (or Qs, fractional) : 5.0000E-01

• **Polarization transmission through 393+Qy**

$\hat{V} = 35\,\text{kV}$ ($\dot{\gamma} \approx 1$) and $\hat{V} = 300\,\text{kV}$ ($\dot{\gamma} = 8.5$)

AVERAGE A FEW INDIVIDUAL PARTICLES

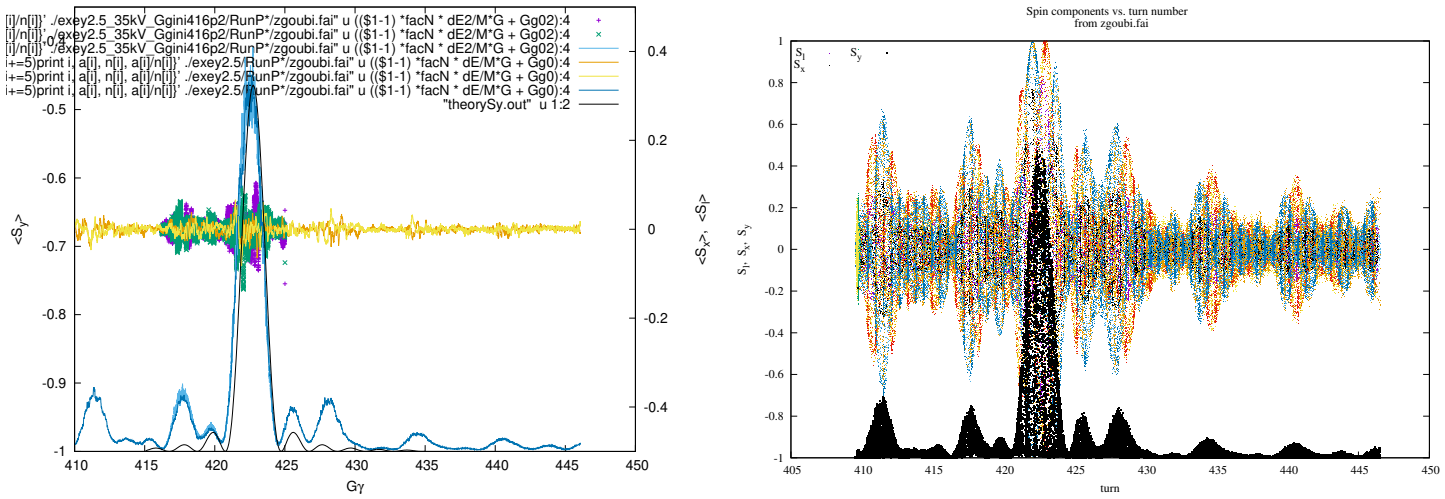

Figure 8: Proton, 2 snakes, $\epsilon_{\mathbf{x}}/\pi = \epsilon_{\mathbf{y}}/\pi = \mathbf{2.5}\,\mu$m. Two crossing speeds: $\dot{\gamma} = 1$ ($\hat{V} = 35\,$kV, $450\,10^3$ turns) and $\dot{\gamma} = 8.5$ ($\hat{V} = 300\,$kV, $120\,10^3$ turns). Left: $< S_y >_{10^3\,\text{particles}}$ versus $G\gamma$; the black curve represents the envelope equation (Eq. 2) for the present strength $|\epsilon_K| = 0.44715$. Right: spin components for a few individual motions, the black curve is the S_y component motion, whereas $S_x,\ S_l$ average to 0. No depolarization observed.

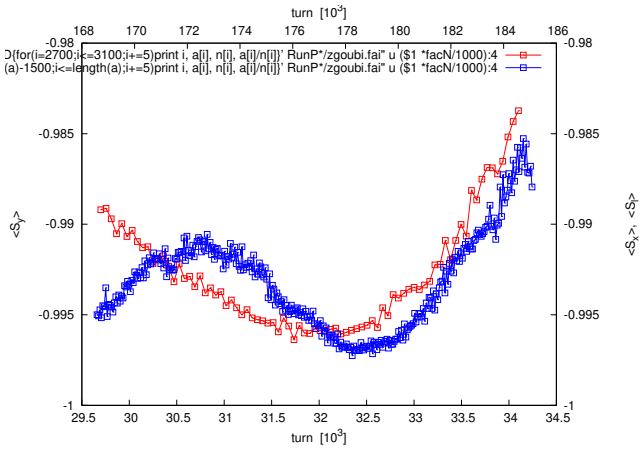

Figure 9: Initial (red, bottom axis) and final (blue, top axis) sections of $\langle S_y \rangle$ (turn) curve of Fig. 8. Essentially no effect of crossing 303+Qy on polarization.

• Introduce 0.6 mm *rms* vertical defect orbit

Random orbit is generated using RHIC V-kickers.

Just 1 random orbit seed tracked ...

Spin matrix at IP6:

```
                Spin transfer matrix, momentum group # 1 :

      -0.999691       -6.607107E-04   -2.486106E-02
      -7.140160E-04   -0.998472        5.524692E-02
      -2.485958E-02    5.524758E-02    0.998163

  Determinant =     1.0000000000
  Trace =    -1.0000000000;  spin precession acos((trace-1)/2) =   179.9996471363 deg
```

Precession axis : (0.012436,-0.027640,-0.999541) -> angle to vertical = 178.2632 deg

Spin precession/2pi (or Qs, fractional) : 5.0000E-01

$\hat{V} = 35\,\mathrm{kV}$ ($\dot{\gamma} \approx 1$) and $\hat{V} = 300\,\mathrm{kV}$ ($\dot{\gamma} = 8.5$)

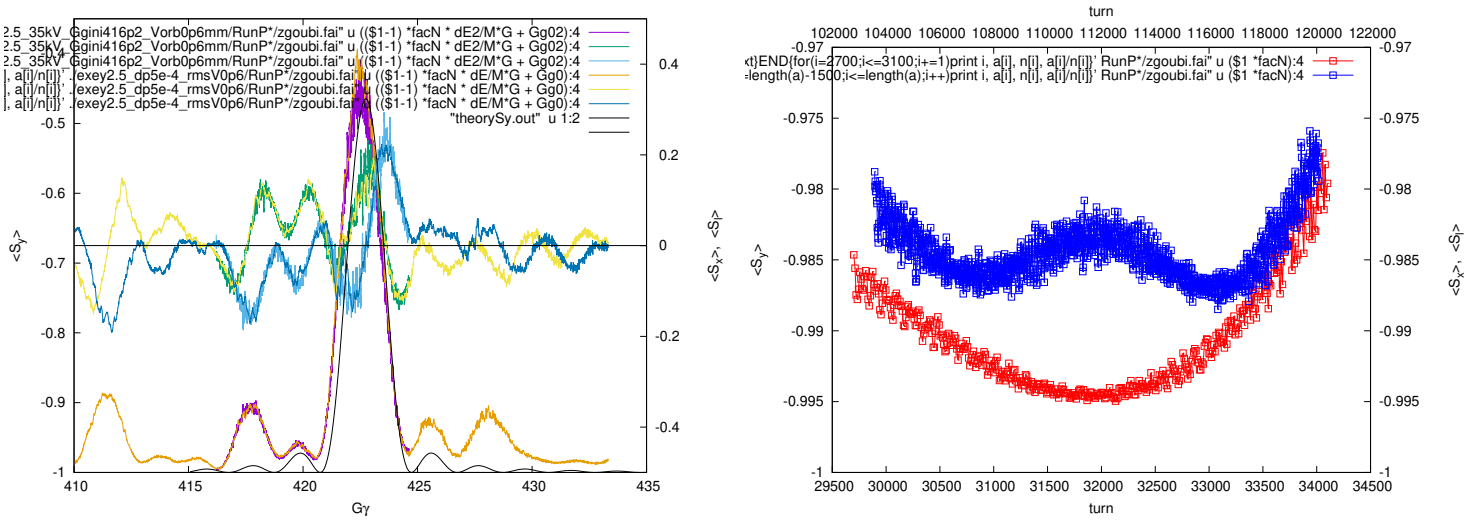

Figure 10: Proton, 2 snakes, $\epsilon_{\mathbf{x}}/\pi = \epsilon_{\mathbf{y}}/\pi = \mathbf{2.5}\,\mu$m, case of 0.61 mm *rms* vertical defect orbit. Just 1 seed. Left: turn-by-turn $\langle S_y \rangle$ (left axis), and $\langle S_l \rangle$ $\langle S_x \rangle$ (right axis) 1,000-particle averages, $\hat{V} = 35\,\mathrm{kV}$ and $300\,\mathrm{kV}$. Right: $\langle S_y \rangle\,(turn)$ in start (red, bottom horizontal axis) and end (blue, top horizontal axis) regions; minimum upstream and downstream $< S_y >$ in this scan differ by $< 1\%$.

Greatest tilt is near resonance: $\langle S_x \rangle \approx 0$; $\langle S_l \rangle \approx -0.55$ $\langle S_y \rangle \approx -0.45$ $\Rightarrow$ tilt with respect to vertical ≈ 50 degrees

• Polarization transmission through neighboring 249-Qy, 255-Qy

Crossing of these two resonances is simulated to check a possible effect of an interference as they are near one another.
$\hat{V} = 35\,\text{kV}$, $\dot{\gamma} \approx 1$, 10^6 turns in this simulation.
Both injection and collision RHIC optics are tracked.

◇ Collision optics:

```
@ Q1 e      0.68502511E+00  28  [frac., int.]
@ Q2        0.67301259E+00  29  [frac., int.]
@ DQ1 e     0.5950653338
@ DQ2      %le      1.344023035
@ BETXMAX  1.91591785E+03
@ BETYMAX  1.85831209E+03
@ BETXMIN   7.09100193E-01
@ BETYMIN   6.95108298E-01
```

Spin transfer matrix (computed at $G\gamma = 210$):

```
    -1.00000          3.109652E-06    7.664872E-06
    -3.109508E-06    -1.00000         1.875454E-05
     7.664931E-06     1.875452E-05    1.00000

Determinant =      1.0000000000
Trace = -1.00;  acos((trace-1)/2) =   179.99982 deg
Precession axis :  (-0.000004,-0.000009,-1.000)
Qs, fractional : 5.0000E-01
```

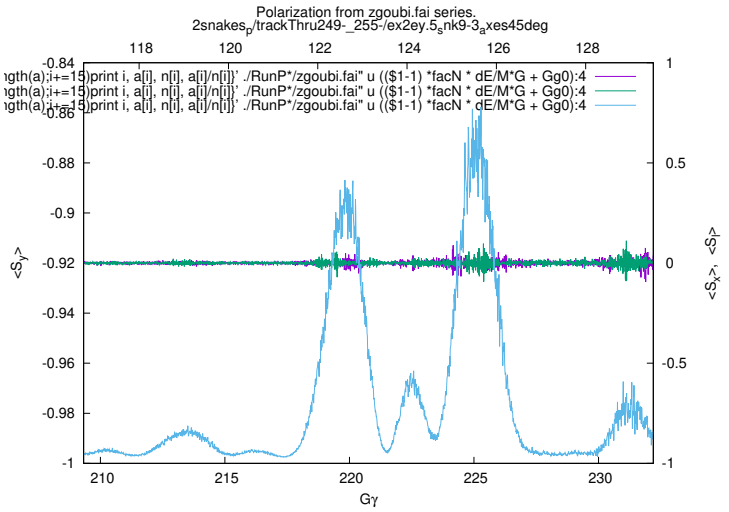

Figure 11: Crossing 249-Qy and 255-Qy, proton, 2 snakes, collision optics, $\epsilon_{\mathbf{x}}/\pi = \epsilon_{\mathbf{y}}/\pi = \mathbf{2.5}\,\mu$m, Closed orbit is zero. Turn-by-turn $\langle S_y \rangle$ (left axis), and $\langle S_l \rangle$ $\langle S_x \rangle$ (right axis), $\hat{V} = 35\,\text{kV}$, 10^6 turns.

Outcome of crossing: no depolarization observed.

◇ Injection optics:

```
@ Q1           0.69740853E+00  28  [frac., int.]
@ Q2           0.68958141E+00  29  [frac., int.]
@ DQ1          2.940417725
@ DQ2          3.543429457
@ BETXMAX/MIN 1.50031929E+02     2.49106616E+00
@ BETYMAX/MIN 1.59863760E+02     3.80495340E+00
```

Graph similar to the above, with smaller max($< S_y >$).

Outcome of crossing: no depolarization observed.

B.1.2 Transverse emittances $\epsilon_x/\pi = \epsilon_y/\pi = 1\,\mu$m

Considering the previous results with $\epsilon_x/\pi = \epsilon_y/\pi = \mathbf{2.5}\,\mu$m, namely marginal effect of crossing speed, then using $\hat{V} = 300\,$kV is fine: tracking is 8 times faster.

• Initial phase-spaces

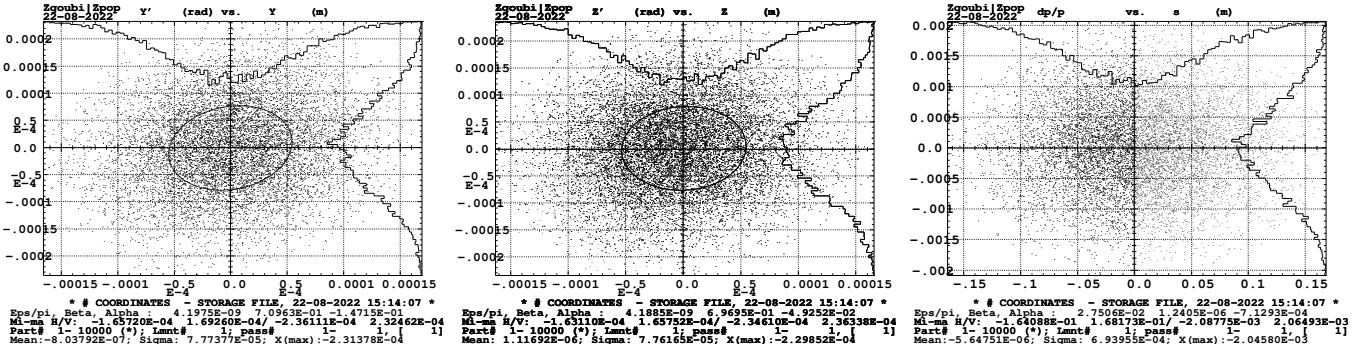

Figure 12: Initial phase spaces, at IP6, matched to lattice: horizontal, vertical, longitudinal (l-dp).

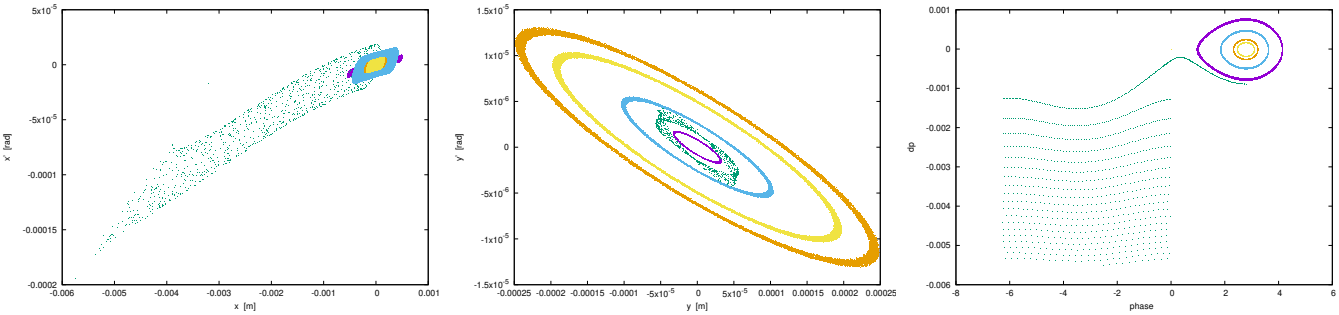

Figure 13: Monitoring: 185,000-turn phase spaces, a few particles (different colors), observation is at 9 o'clock snake. Incidentally, a particle is beyond momentum acceptance here.

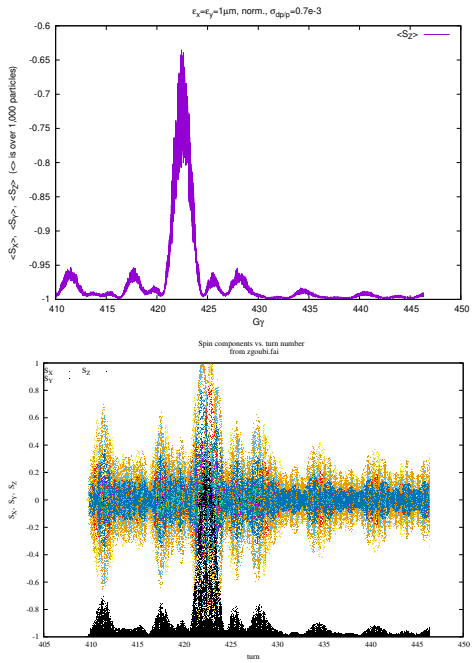

Figure 14: Top: Average S_y. Bottom: spin components for a few individual motions.

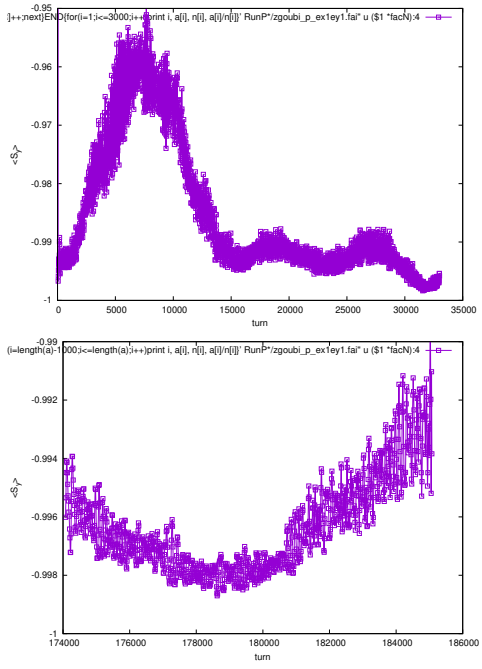

Figure 15: Initial (top) and final (bot.) section of $\langle S_y \rangle\,(\text{turn})$ curve of Fig. 14. There is no obvious sign of polarization loss.

• **Introduce 0.6 mm *rms* vertical defect orbit**

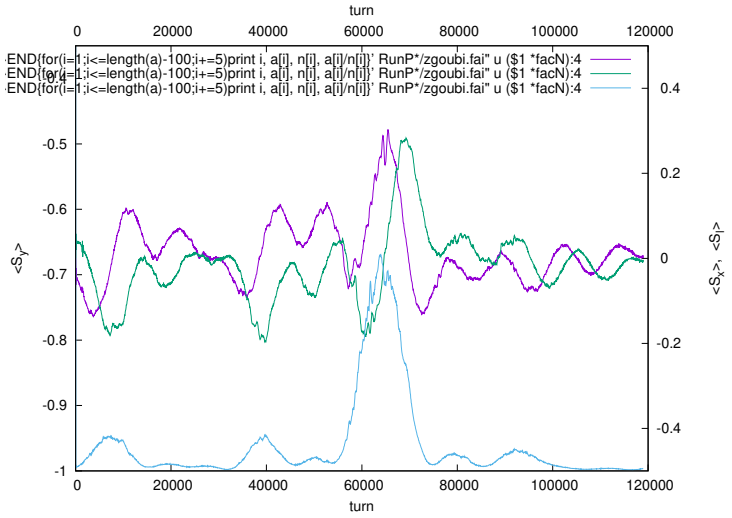

Figure 16: Proton, $\epsilon_{\mathbf{x}}/\pi = \epsilon_{\mathbf{y}}/\pi = \mathbf{1}\,\mu$m, case of 0.61 mm *rms* vertical defect orbit. Just 1 seed. Turn-by-turn $\langle S_y \rangle$ (left axis), and $\langle S_l \rangle$ $\langle S_x \rangle$ (right axis) 1,000-particle averages. Difference between upstream and downstream min$(< S_y >)$ is marginal.

B.1.3 Transverse emittances $\epsilon_x/\pi = 2\,\mu$m, $\epsilon_y/\pi = 0.5\,\mu$m

Considering the previous results with $\epsilon_x/\pi = \epsilon_y/\pi = 2.5\,\mu$m - marginal effect of crossing speed on $< S_y > (G\gamma)$ envelop - use fast tracking, $\hat{V} = 300\,$kV.

- **Initial phase-spaces**

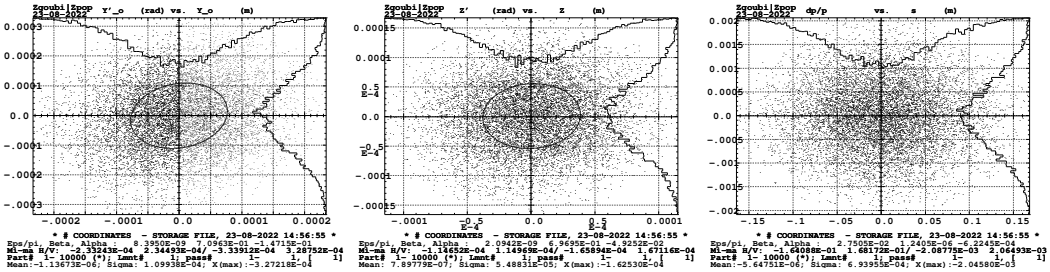

Figure 17: Initial phase spaces, at IP6, matched to lattice: horizontal, vertical, longitudinal (l-dp).

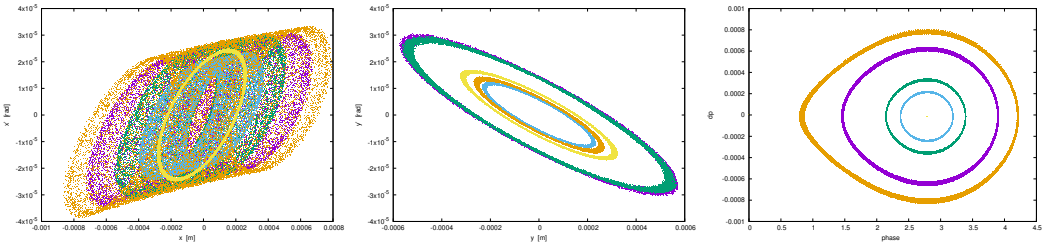

Figure 18: Monitoring: 185,000-turn phase spaces, a few particles (different colors), observation is at 9 o'clock snake. Horizontal oscillation of ± 1 mm (left graph) is for $dp/p \approx 10^{-3}$ excursion (right) hence a local dispersion at 9 o'clock snake of about 1 m.

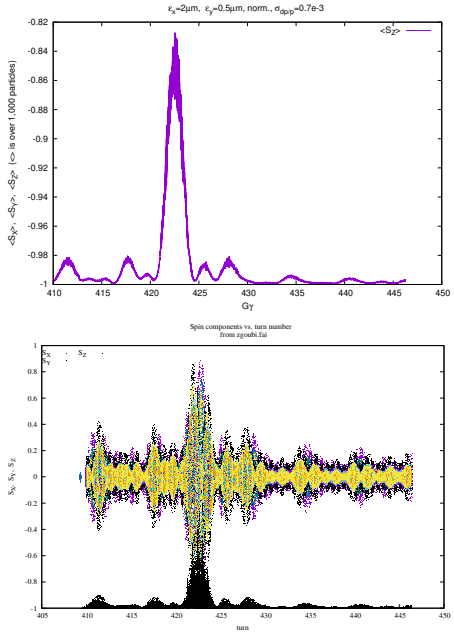

Figure 19: Top: Average S_y. Middle: average S_y, S_l and S_x.
Bottom: spin components for a few individual motions.

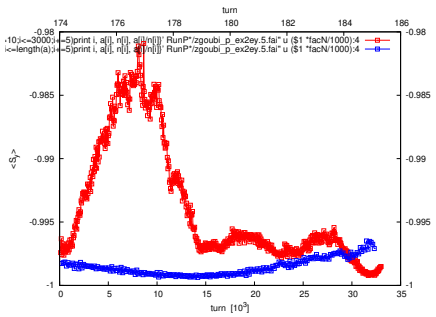

Figure 20: Initial (red, bottom axis) and final (blue, top axis) sections of $\langle S_y \rangle$ (turn) curve of Fig. 19.

• **Introduce 0.3 mm *rms* vertical defect orbit**

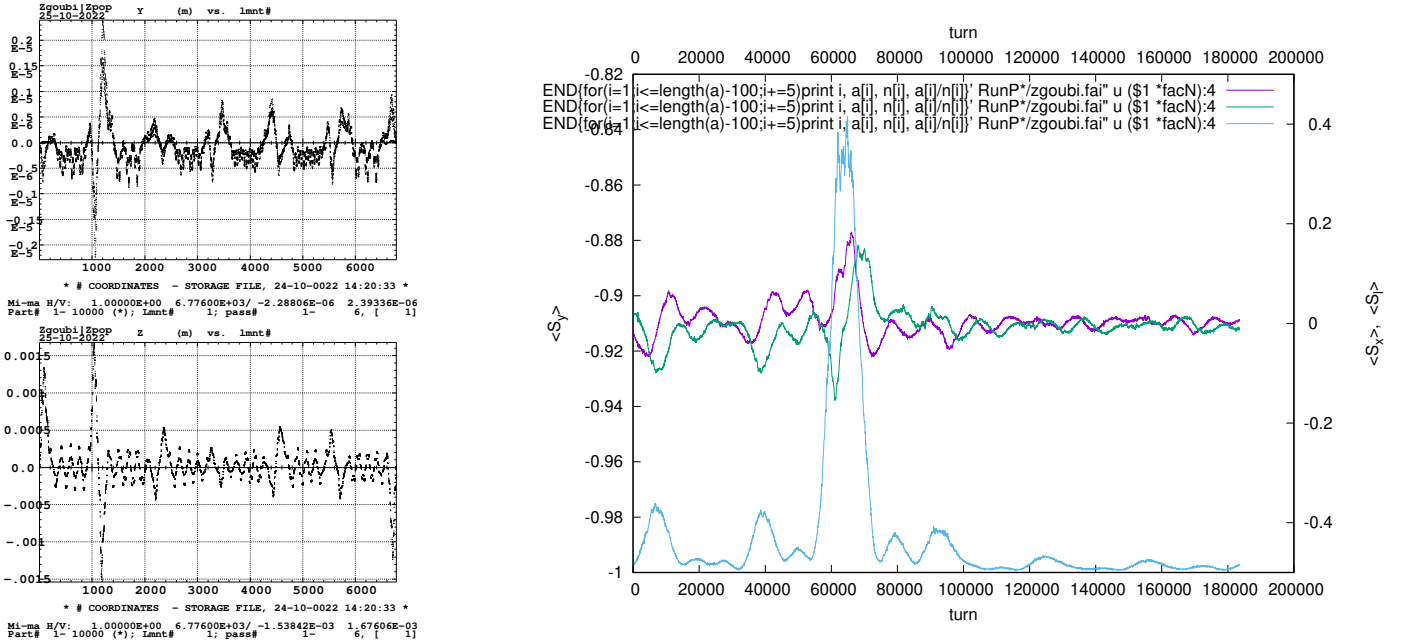

Figure 21: Proton, $\epsilon_{\mathbf{x}}/\pi = \mathbf{2}\,\mu$m, $\epsilon_{\mathbf{y}}/\pi = \mathbf{0.5}\,\mu$m, case of 0.302 mm *rms* vertical defect orbit. Just 1 seed. Left: x orbit, quasi-zero (top) and y orbit, 0.302 mm *rms* (bottom), 5 turns superposed here, as a sanity check. Right: turn-by-turn $\langle S_y\rangle$, $\langle S_l\rangle$ and $\langle S_x\rangle$ 1,000-particle averages.

• **Introduce 0.6 mm *rms* vertical defect orbit**

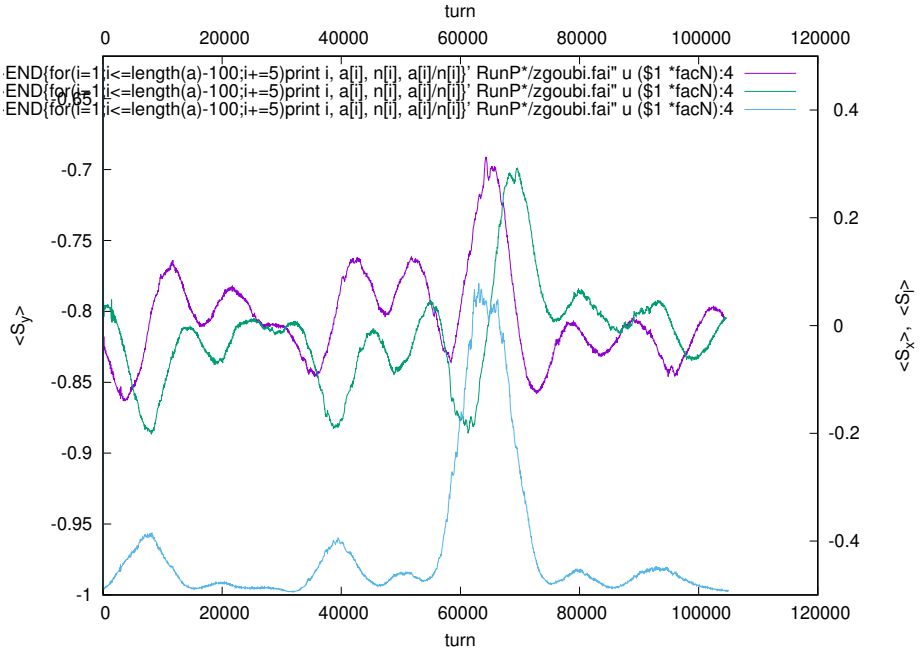

Figure 22: Proton, $\epsilon_{\mathbf{x}}/\pi = \mathbf{2}\,\mu$m, $\epsilon_y/\pi = 0.5\,\mu$m, case of 0.61 mm *rms* vertical defect orbit. Just 1 seed. Turn-by-turn $\langle S_y\rangle$ (left axis), and $\langle S_l\rangle$ $\langle S_x\rangle$ (right axis) 1,000-particle averages. Polarization difference in start and end regions is $< 1\%$.

B.2 Case of RHIC with EIC HSR fractional tunes

Optical data are detailed in Fig. 2 and Tab. 3, resonance strength spectrum is given in Fig. 5.

B.2.1 Transverse emittances $\epsilon_{\mathbf{x}}/\pi = \epsilon_{\mathbf{y}}/\pi = \mathbf{2.5}\,\mu$m.

• Crossing 393+Qy

◇ Qx/Qy=28.228/29.21

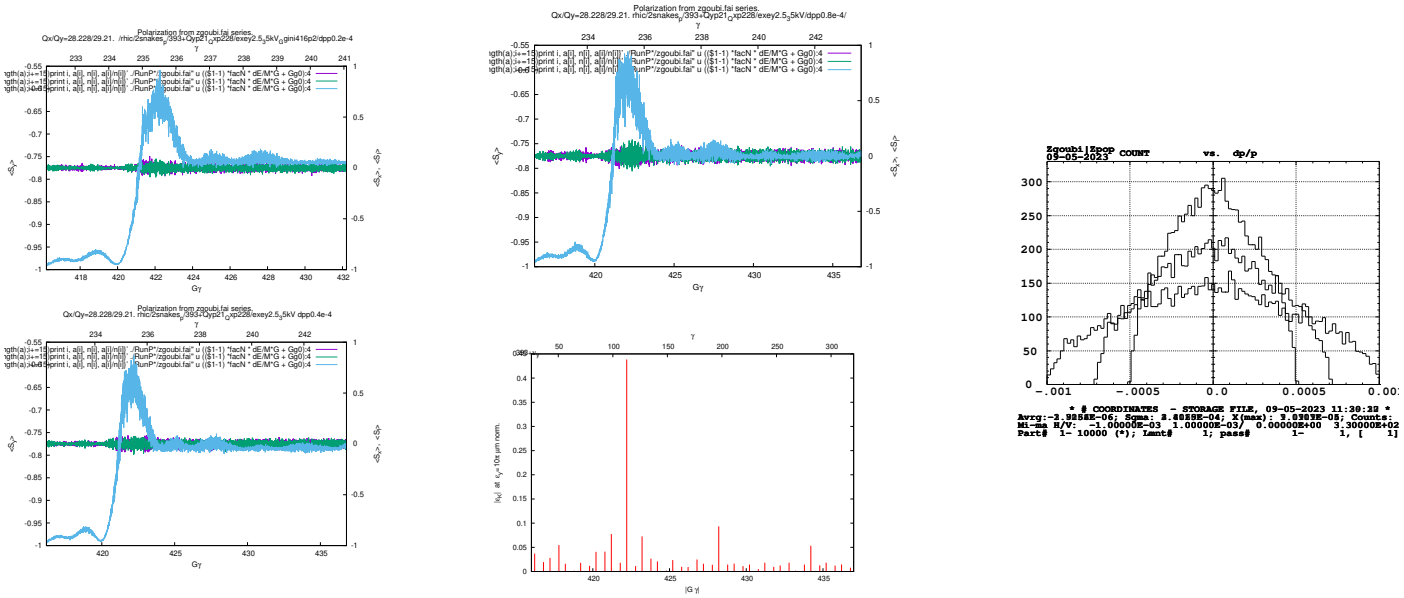

Figure 23: Proton, $\epsilon_{\mathbf{x}}/\pi = \epsilon_{\mathbf{y}}/\pi = \mathbf{2.5}\,\mu$m, xing 393+29.21, $\dot{\gamma} \approx 1$/s ($\hat{V} = 35$ kV). Case of Qx/Qy=28.228/29.21. Left column and middle top graph: dp/p 0.2e-4, 0.4e-4 and 0.8e-4. Middle col. bottom: local resonance spectrum (a zoom-in from Fig. 5), spectral lines show concordance with the $< S_y > (G\gamma)$ graph above. Right: dp/p distributions used, 0.2e-4, 0.4e-4, 0.8e-4;

◇ Qx/Qy=28.228/29.17

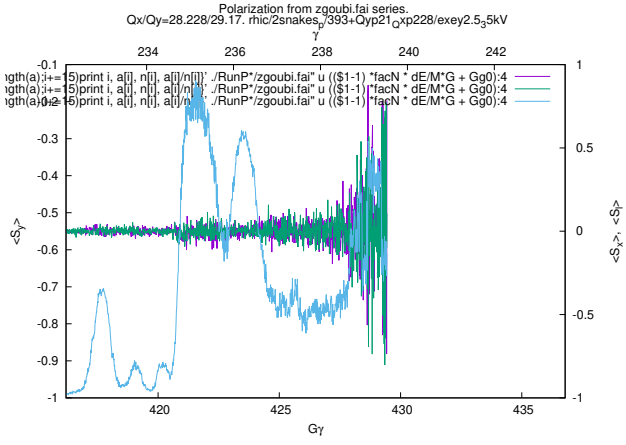

Figure 24: Proton, $\epsilon_{\mathbf{x}}/\pi = \epsilon_{\mathbf{y}}/\pi = \mathbf{2.5}\,\mu$m, xing 411-29.19, $\dot{\gamma} \approx 1$/s ($\hat{V} = 35$ kV, 9×10^5 turns). Case of Qx/Qy=28.228/29.19

- **Crossing 411-Qy**
  - ◇ **Qx/Qy=28.228/29.21**

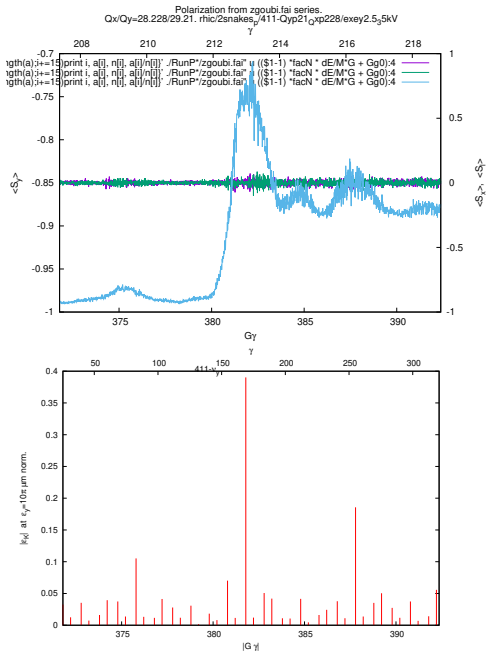

Figure 25: Proton, $\epsilon_{\mathbf{x}}/\pi = \epsilon_{\mathbf{y}}/\pi = \mathbf{2.5}\,\mu$m, xing 411-29.21, $\dot{\gamma} \approx 1$/s ($\hat{V} = 35$ kV). Bottom plot: corresponding resonance spectrum interval from Fig. 5.

  - ◇ **Qx/Qy=28.228/ 29.19**

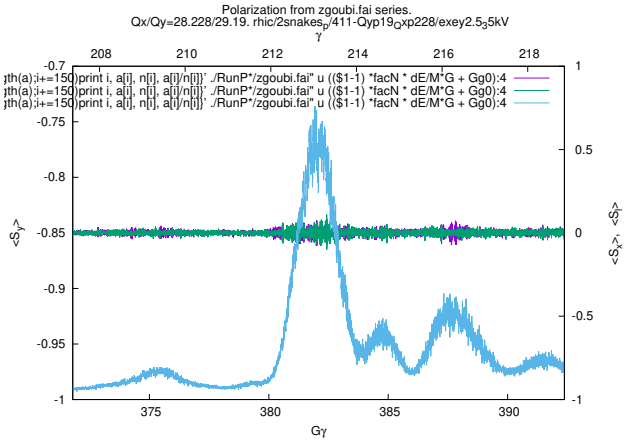

Figure 26: Proton, $\epsilon_{\mathbf{x}}/\pi = \epsilon_{\mathbf{y}}/\pi = \mathbf{2.5}\,\mu$m, xing 411-29.19, $\dot{\gamma} \approx 1$/s ($\hat{V} = 35$ kV). Case of Qx/Qy=28.228/29.19

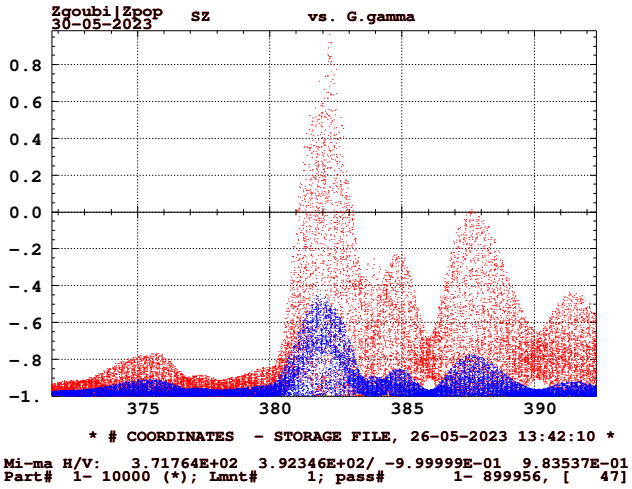

Figure 27: Two individual trajectories (particles differ by invariant value and initial momentum offset).

C Helion, 2 snakes

RF tracking data

They are the following, case of 35 kV peak voltage (peak voltage may be changed, as specified in due place):

```
6769  Keyword, label(s) :  CAVITE      accelerating          cavity

            Accelerating cavity. Type is :   OPTION 2

                 Orbit  length                     =     3.83384593E+03 m
                 RF  harmonic h                    =     3.60000000E+02
                 Peak  voltage                     =     3.50000000E+04 V
                 f_rev * h                         =     2.81502102E+07 Hz
                 Synchronous  phase                =     2.79252680E+00 rd
                 Isochronous  time                 =     1.27885368E-05 s
                 particle charge (Q/QE)            =     2.00000000E+00
                 Q*V*sin(phi_s)                    =     2.39414100E-02 MeV
                 cos(phi_s)                        =    -9.39692621E-01
                 Nu_s/sqrt(alpha) = gamma_tr*nu_s  =     2.75090929E-03
                 dp-acc*sqrt(alpha)                =     1.13887997E-05
                 dgamma/dt                         =     6.66619646E-01 /s
                 rho*dB/dt                         =     3.12237509E+00 T.m/s
                 SR loss, this pass                =     0.00000000E+00 MeV
                 Cavity azimuth        s           =     3.83384603E+05 m
```

C.1 Transverse emittances $\epsilon_x/\pi = \epsilon_y/\pi = 2.5\,\mu$m, for reference

This case is tracked for reference, to permit comparison with different emittance cases in the next Sections. Initial phase-spaces, except for emittance values, are similar to proton case, Fig. 6.

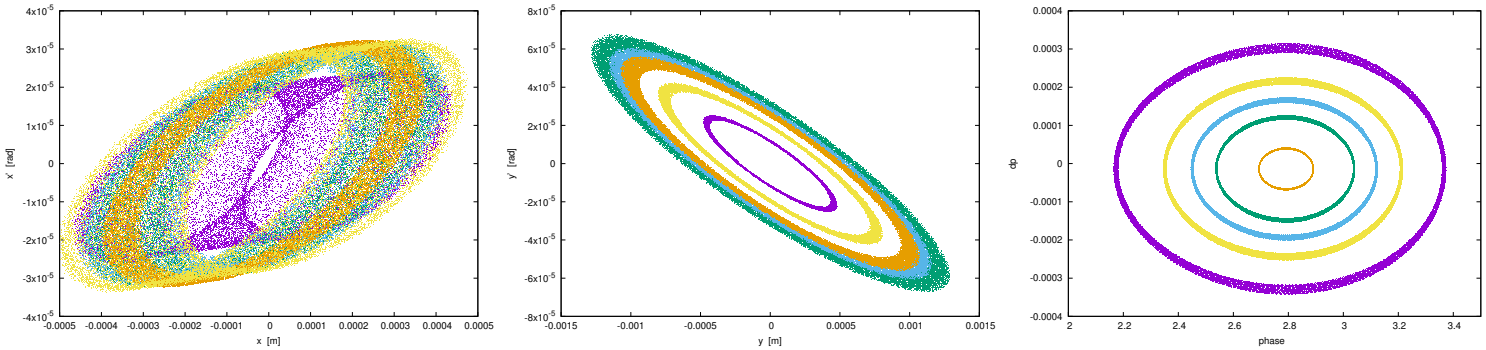

Figure 28: Monitoring: 185,000-turn phase spaces, a few particles (different colors), observation is at 9 o'clock snake. Incidentally, a particle is beyond momentum acceptance here.

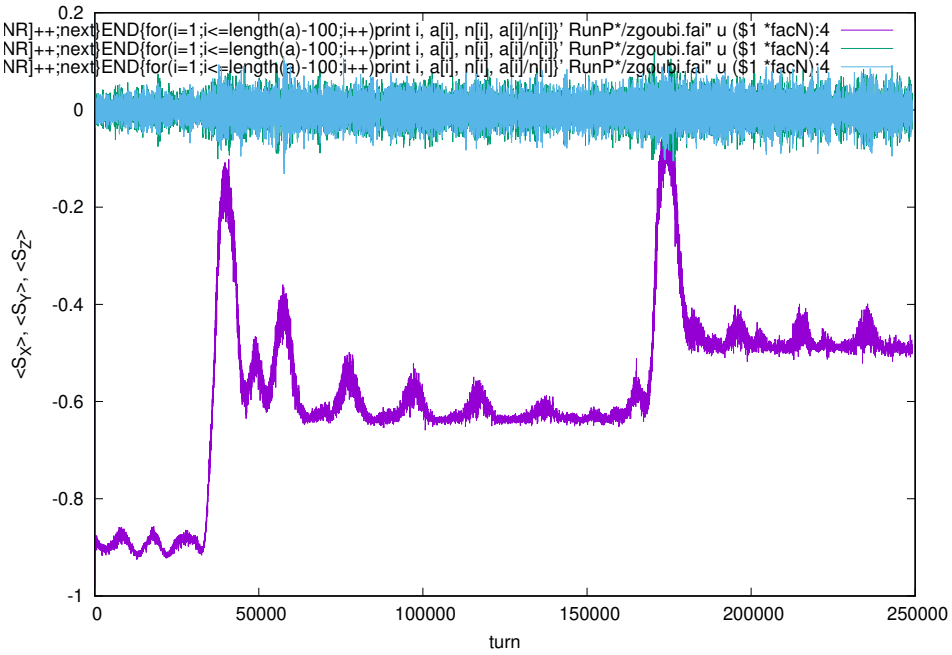

Figure 29: Helion, turn-by-turn $\langle S_y \rangle$, $\langle S_l \rangle$ and $\langle S_x \rangle$ 1,000 particle averages across 735-ν_y and 717+ν_y, helion, $\epsilon_x/\pi = \epsilon_y/\pi = 2.5\,\mu$m normalized. $\hat{V} = 300\,$kV ($\dot{\gamma} = 6$), no need to check 35 kV.

C.2 Transverse emittances $\epsilon_x/\pi = \epsilon_y/\pi = 1\,\mu$m

Initial phase-spaces, except for emittance values, are similar to proton case, Fig. 6.

Current phase-spaces, except for the different emittances, are similar to Fig. 28 case.

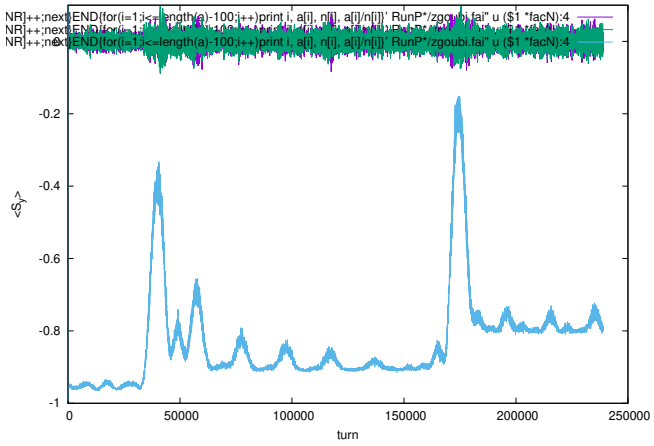

Figure 30: Turn-by-turn $\langle S_y\rangle$, $\langle S_l\rangle$ and $\langle S_x\rangle$ 1,000 particle averages across 735-ν_y and 717+ν_y, helion, $\epsilon_x/\pi = \epsilon_y/\pi = 1\,\mu$m normalized. $\hat{V} = 300$ kV ($\dot{\gamma} = 6$).

C.3 Transverse emittances $\epsilon_x/\pi = 2\,\mu$m, $\epsilon_y/\pi = 0.5\,\mu$m

Initial phase-spaces, except for emittance values, are similar to proton case, Fig. 6.

Current phase-spaces, except for the different emittances, are similar to Fig. 28 case.

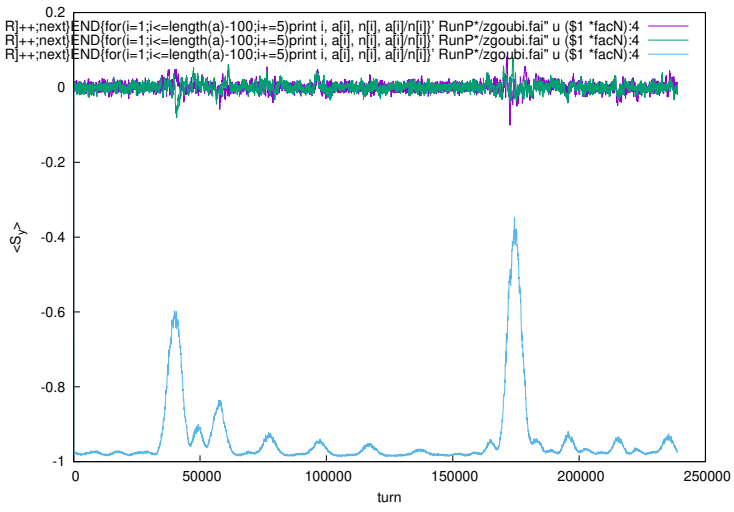

Figure 31: Turn-by-turn $\langle S_y\rangle$, $\langle S_l\rangle$ and $\langle S_x\rangle$ 1,000 particle averages across 735-ν_y and 717+ν_y, helion, $\epsilon_x/\pi = 2\,\mu$m, $\epsilon_y/\pi = 0.5\,\mu$m normalized.

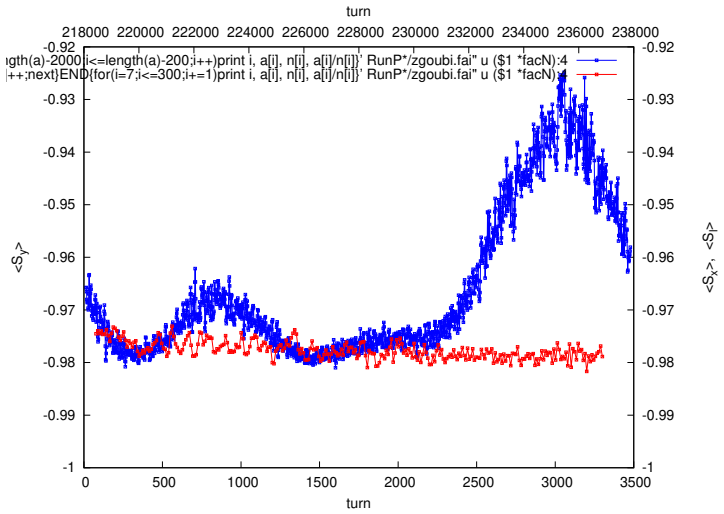

Figure 32: Initial (red) and final (blue) regions of $\langle S_y\rangle$ (turn) curve of Fig. 31. No obvious indication of any polarization loss.

D Helion, 6 snakes

D.1 Transverse emittances $\epsilon_x/\pi = \epsilon_y/\pi = 2.5\ \mu$m, for reference

This case is tracked for reference, to permit comparison with different emittance cases in the next Sections.

• Initial phase-spaces

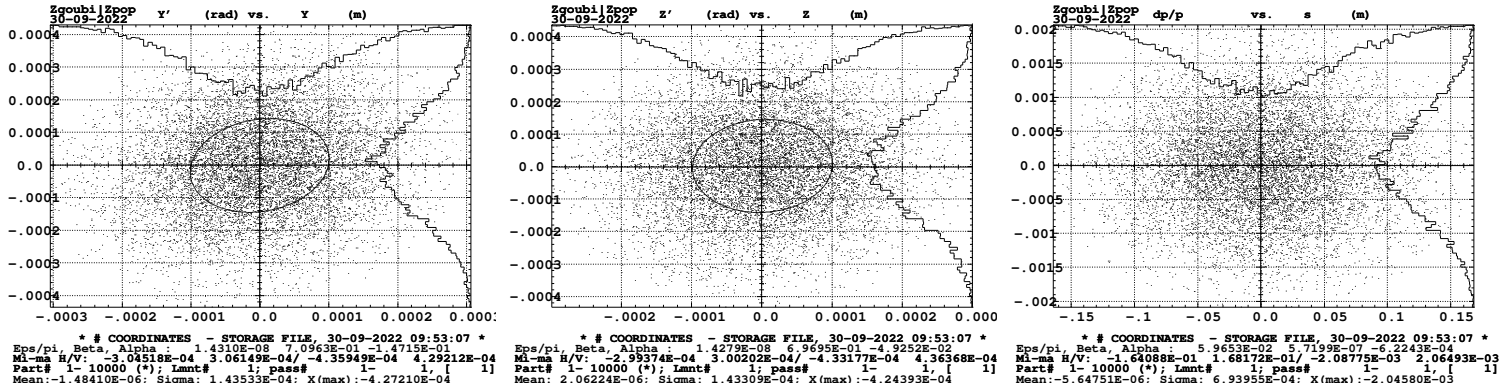

Figure 33: Initial phase spaces, at IP6: horizontal and vertical matched to lattice, longitudinal (l-dp).

• Multiturn monitoring, phase spaces

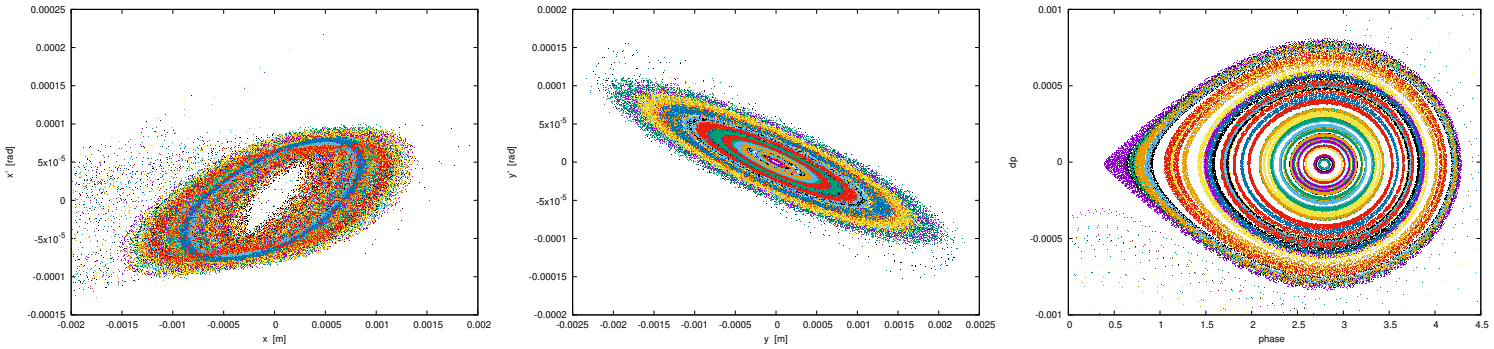

Figure 34: Monitoring: graphs are for 185,000-turn every other 3 turns; 300 particles over the 1,000 tracked (different colors); observation is at 9 o'clock snake.

• Helion, 6 snakes, polarization transmission

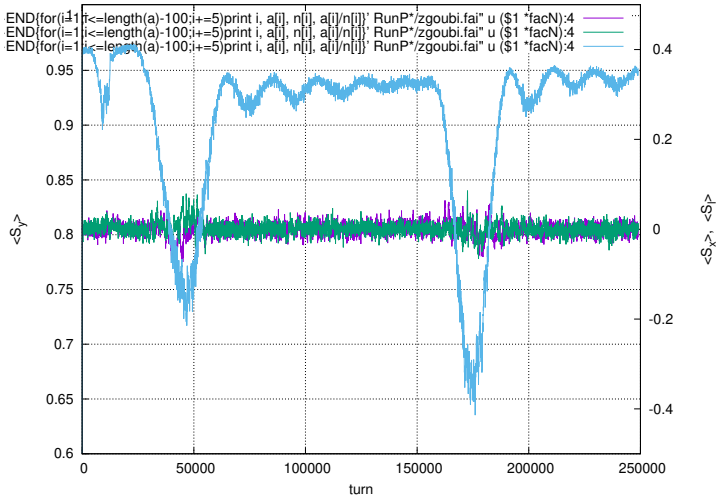

Figure 35: $\hat{V} = 300\,\text{kV}$. Turn-by-turn $\langle S_y \rangle$, $\langle S_l \rangle$ and $\langle S_x \rangle$ 1,000 particle averages across 735-ν_y and 717+ν_y, helion, $\epsilon_x/\pi = \epsilon_y/\pi = 2.5\,\mu$m normalized.

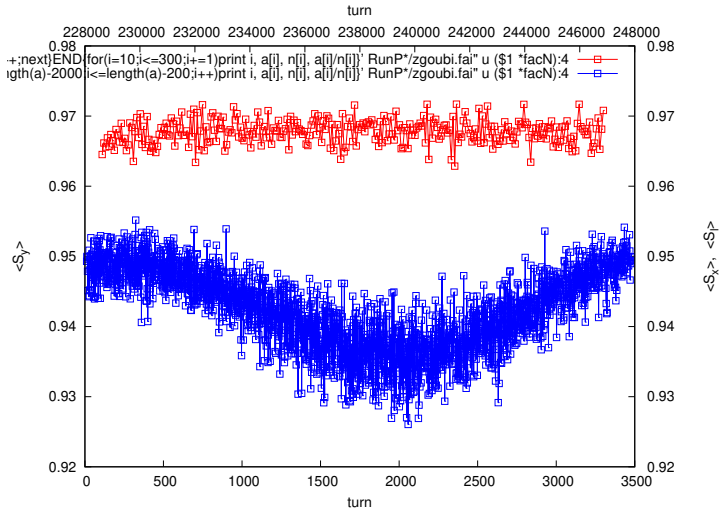

Figure 36: $\hat{V} = 300\,\text{kV}$. Initial (red, bottom and left axes) and final (blue, top and right axes) sections of $\langle S_y \rangle$ (turn) curve of Fig. 35. About 1.8% polarization difference observed, between start and end troughs.

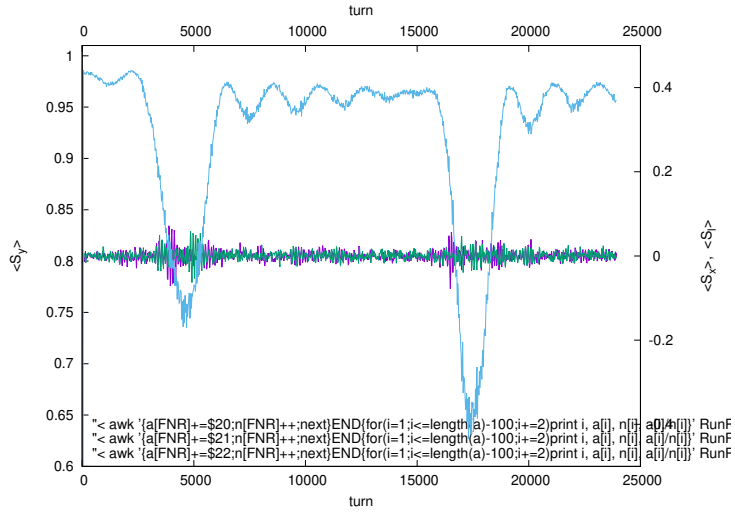

Figure 37: $\hat{V} = 600\,\text{kV}$. Turn-by-turn $\langle S_y \rangle$, $\langle S_l \rangle$ and $\langle S_x \rangle$ 1,000 particle averages across 735-ν_y and 717+ν_y, helion, $\epsilon_x/\pi = \epsilon_y/\pi = 2.5\,\mu$m normalized.

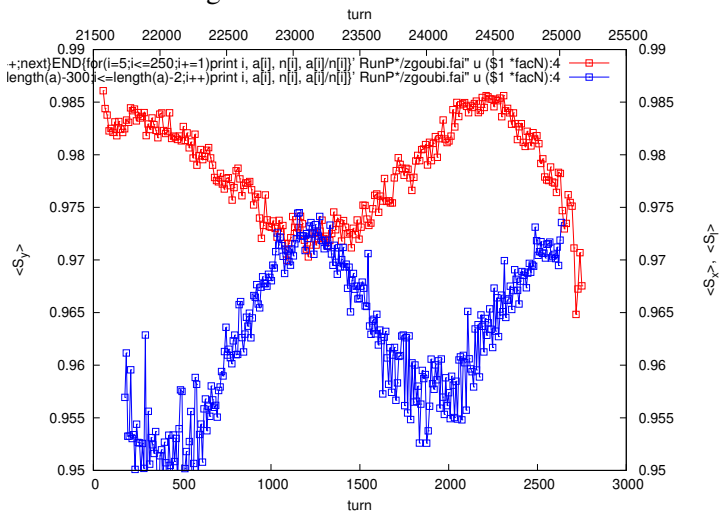

Figure 38: $\dot{\gamma} = 17$. Initial (red, bottom and left axes) and final (blue, top and right axes) sections of $\langle S_y \rangle$ (turn) curve of Fig. 37. About 1.3% polarization difference observed, between start and end troughs.

I do not have random orbit simulation.

D.2 Transverse emittances $\epsilon_x/\pi = \epsilon_y/\pi = 1\,\mu$m

Initial phase-spaces, except for emittance values, are as in Fig. 33, motion phase spaces are as in Fig. 34.

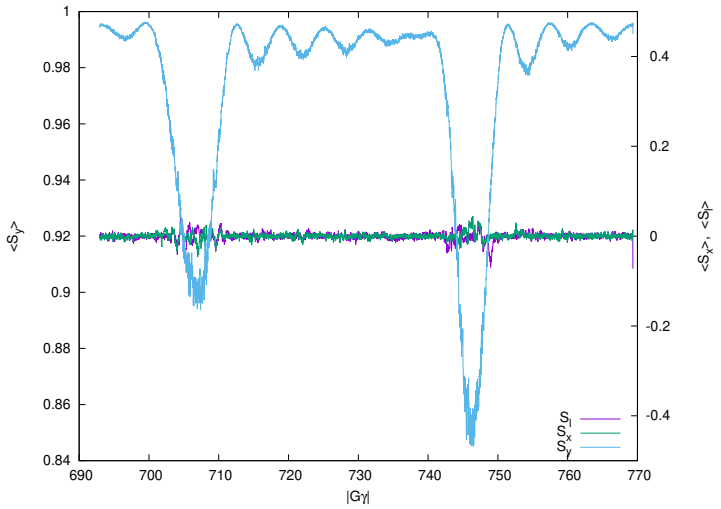

Figure 39: Turn-by-turn $\langle S_y\rangle$, $\langle S_l\rangle$ and $\langle S_x\rangle$ 1,000 particle averages across 735-ν_y and 717+ν_y, helion. $\nu_y = 29.6730$. $\epsilon_x/\pi = \epsilon_y/\pi = 2.5\,\mu$m normalized. $\hat{V} = 300\,$kV, $\phi_s = 2.7925$, $\dot{\gamma} = 6\,$/s

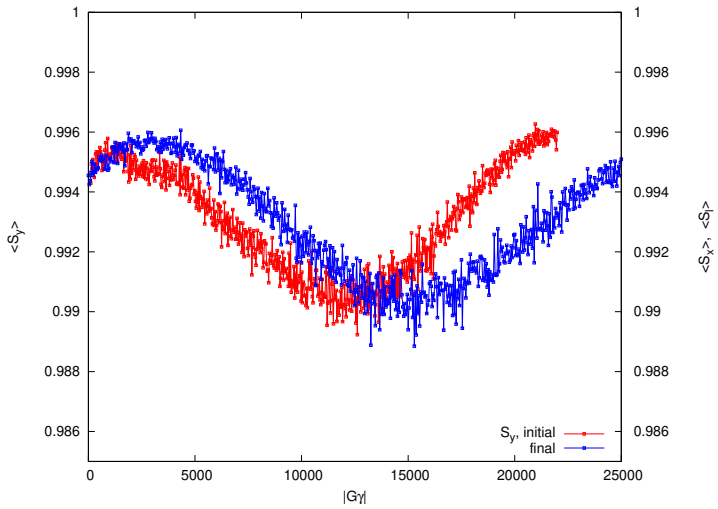

Figure 40: Initial (red, bottom and left axes) and final (blue, top and right axes) sections of $\langle S_y\rangle$ (turn) curve of Fig. 39. No obvious polarization loss observed.

I do not have random orbit simulation.

D.3 Transverse emittances $\epsilon_x/\pi = 2\,\mu$m, $\epsilon_y/\pi = 0.5\,\mu$m

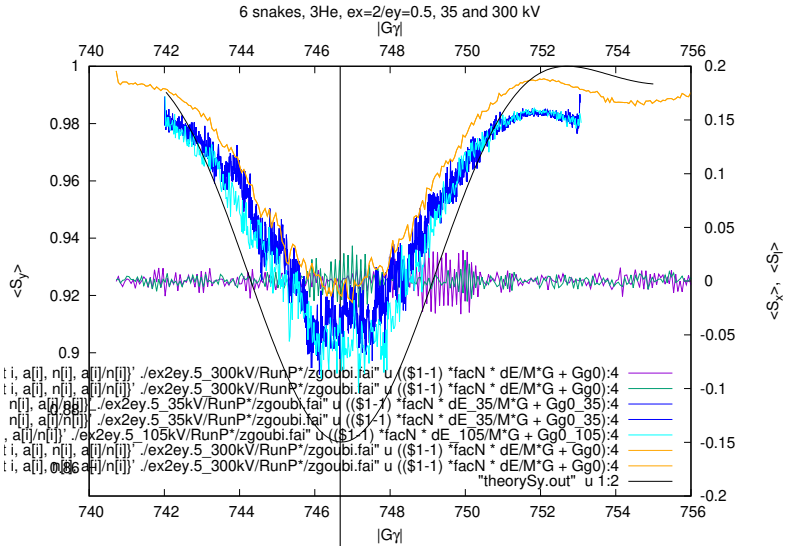

Figure 41: 3He, 6 snakes, $\epsilon_x/\pi = 2\,\mu$m, $\epsilon_y/\pi = 0.5\,\mu$m. Turn-by-turn $\langle S_y\rangle$, $\langle S_l\rangle$ and $\langle S_x\rangle$ 500-particle averages. Blue, orange and cyan: 35 kV (blue), 105 kV (cyan) and 300 kV (orange) cases. Vertical bar: location of the intrinsic resonance $G\gamma_{\rm res} = 717 + \nu_y = 746.673$. Black curve: theoretical envelope (Eq. 2).

• Introduce 0.6 mm *rms* vertical defect orbit

Just 1 random defect orbit seed tracked ...

Spin matrix at IP6:

```
             Spin transfer matrix, momentum group # 1 :

 -0.970857       -4.664780E-02    0.235074
 -9.283768E-02   -0.831086       -0.548340
  0.220945       -0.554184        0.802535
```

Precession axis : (-0.120104, 0.290382,-0.949344) -> angle to vertical is 161.6851 deg
Spin precession/2pi (or Qs, fractional) : 4.9613E-01

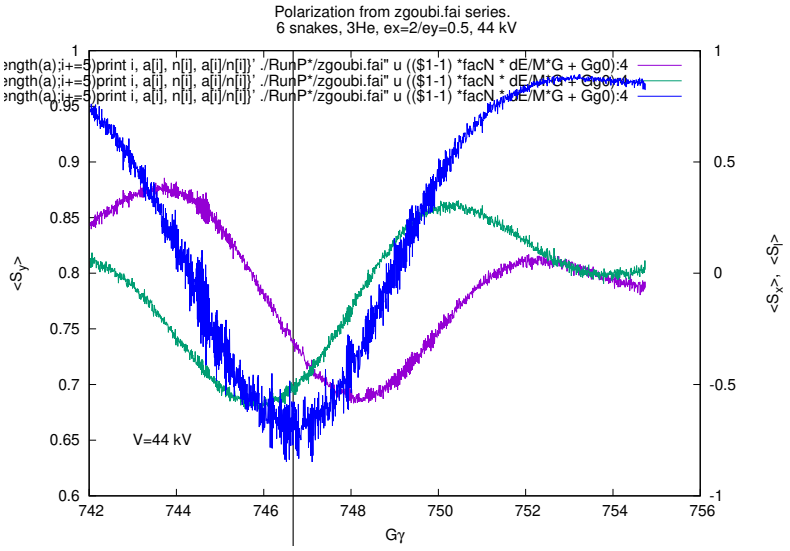

Figure 42: 3He, 6 snakes, $\epsilon_x/\pi = 2\,\mu$m, $\epsilon_y/\pi = 0.5\,\mu$m. case of 0.61 mm *rms* vertical defect orbit. Turn-by-turn $\langle S_y\rangle$, and theoretical envelop (left axis), and $\langle S_l\rangle$ $\langle S_x\rangle$ (right axis) 500-particle averages, $\hat{V} = 44$ kV.

E Helion, 4 snakes

• Two configurations have been simulated, which allow energy-independent spin tune:

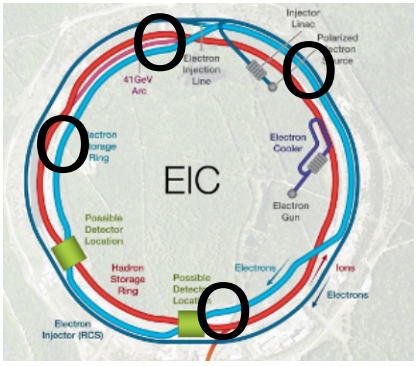

- snakes located at 9 o'clock, 11, 1 and 5

- snakes located at 7 o'clock, 9, 11 and 3

Both configurations ensure
$\theta_{1-2} + \theta_{3-4} = \theta_{2-3} + \theta_{4-1} = \pi$

Axes orientation ϕ_k ensures half-integer spin tune
$\nu_{sp} = \frac{1}{\pi} \sum_{k=1}^{4} (-)^k \phi_k$

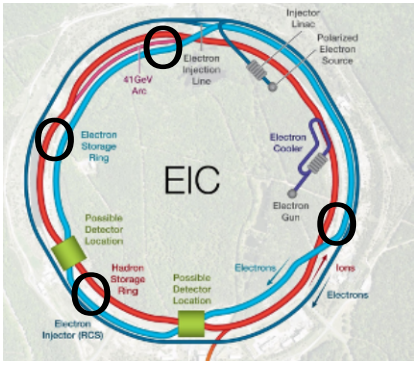

• **These two 4-snake configurations have been reproduced using RHIC lattice**

Check orbital spacing of snakes around the ring in RHIC lattcie model:

```
lmnt#     93   SNK1   -1.00285 93     2*pi+%-(635) ->  0.333335802 *pi
lmnt#    201   SNK2   -2.05004 201    % - %%   ->  -0.3333309297
lmnt#    309   SNK3   -3.09724 309    % - %%   ->  -0.3333341128
lmnt#    417   SNK4   -4.14444 417    % - %%   ->  -0.3333341128
lmnt#    527   SNK5   -5.19164 527    % - %%   ->  -0.3333341128
lmnt#    635   SNK6   -6.23883 635    % - %%   ->  -0.3333309297
```

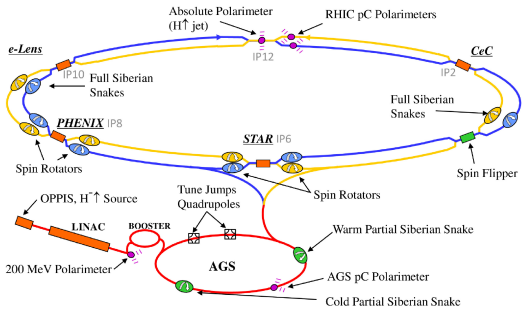

E.1 Transverse emittances $\epsilon_x/\pi = \epsilon_y/\pi = 2.5\,\mu$m

• snakes(axis angle) at
7(+22.5)-9(-22.5)-11(+22.5)-3(-22.5) o'clock
voltage 70kV ($\dot{\gamma} = 1.4$)

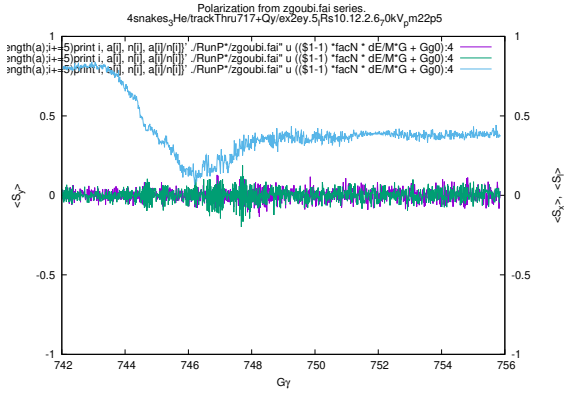

Figure 43: Turn-by-turn $\langle S_y\rangle$, $\langle S_l\rangle$ and $\langle S_x\rangle$ 1,000 particle averages across 717+ν_y, helion. No vertical orbit.

• snakes(axis angle) at
9(+22.5)-11(-22.5)-1(+22.5)-5(-22.5) o'clock
voltage 70kV ($\dot{\gamma} = 1.4$)

No defect

Spin matrix at IP6:

```
      Spin transfer matrix, momentum group # 1 :

 -0.965723         0.136746        -0.220633
 -4.207839E-02    -0.921213        -0.386778
 -0.256140        -0.364236         0.895390

Trace =    -0.9915454149;  spin precession = 174.7298631678 deg
```

Precession axis : (0.12270, 0.19328,-0.97343) -> 166.7651 deg
Spin precession/2pi (or Qs, fractional) : 4.8536E-01

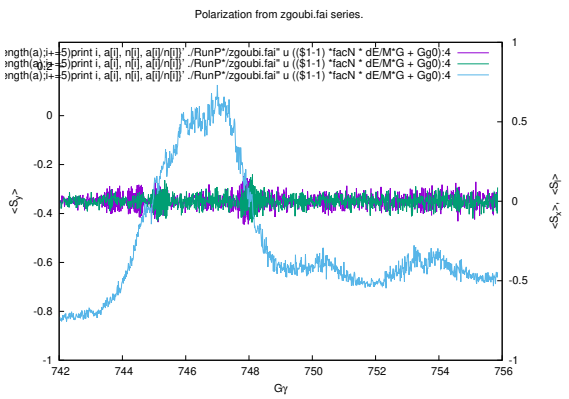

Vertical orbit defect 0.6 mm rms

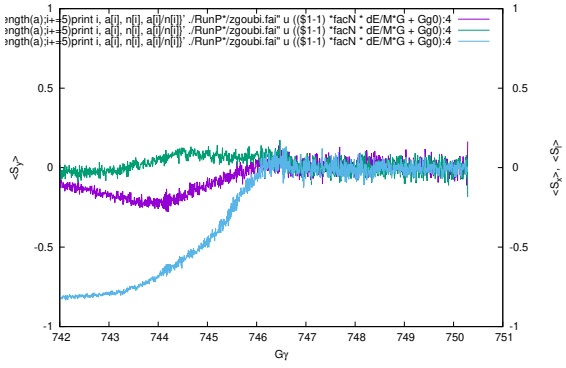

Figure 44: Turn-by-turn $\langle S_y\rangle$, $\langle S_l\rangle$ and $\langle S_x\rangle$ 1,000 particle averages across 717+ν_y, helion.

E.2 Transverse emittances $\epsilon_x/\pi = 2\,\mu$m, $\epsilon_y/\pi = 0.5\,\mu$m

• snakes(axis angle)
at 7(+22.5)-9(-22.5)-11(+22.5)-3(-22.5) o'clock (top S_y curve)
and at 9(+22.5)-11(-22.5)-1(+22.5)-5(-22.5) o'clock (bot. S_y curve)
Voltages are 300 kV (top) and 70 kV (bottom).

• snakes(axis angle) at
9(+45)-11(0)-1(+45)-5(0) o'clock
voltage 70kV

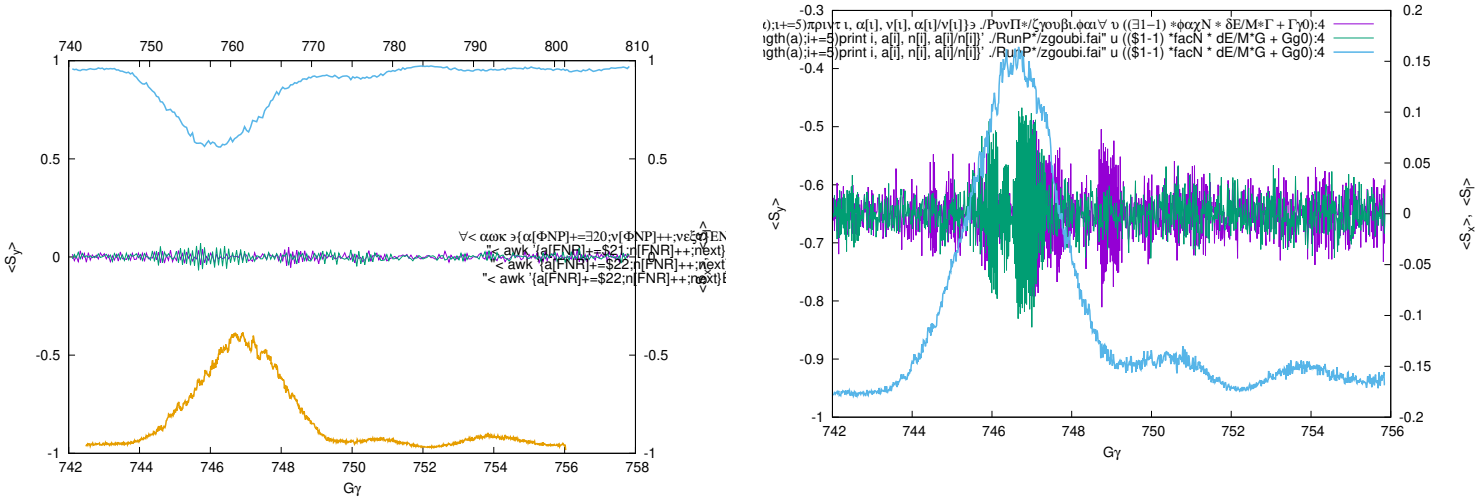

Figure 45: Turn-by-turn $\langle S_y \rangle$, $\langle S_l \rangle$ and $\langle S_x \rangle$ 1,000 particle averages across 717+ν_y, helion.

• snakes(axis angle) at
9(+22.5)-11(-22.5)-1(+22.5)-5(-22.5) o'clock
voltage 70kV

No defect

Vertical orbit defect 0.6 mm rms

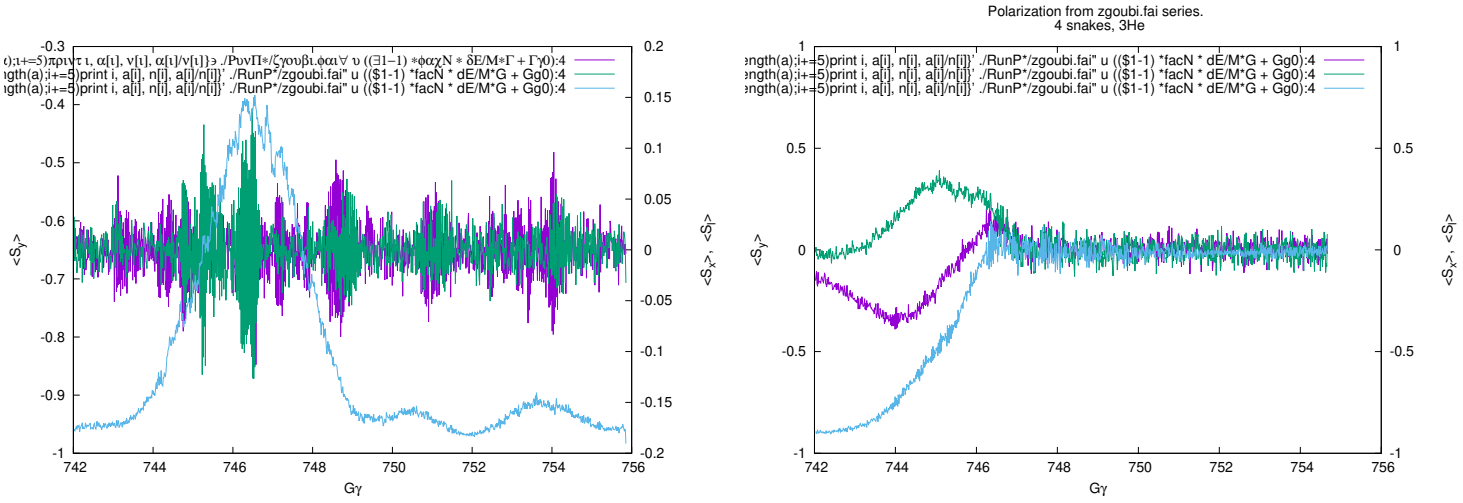

Figure 46: Turn-by-turn $\langle S_y \rangle$, $\langle S_l \rangle$ and $\langle S_x \rangle$ 1,000 particle averages across 717+ν_y, helion.

Vertical orbit defect 0.2 mm rms

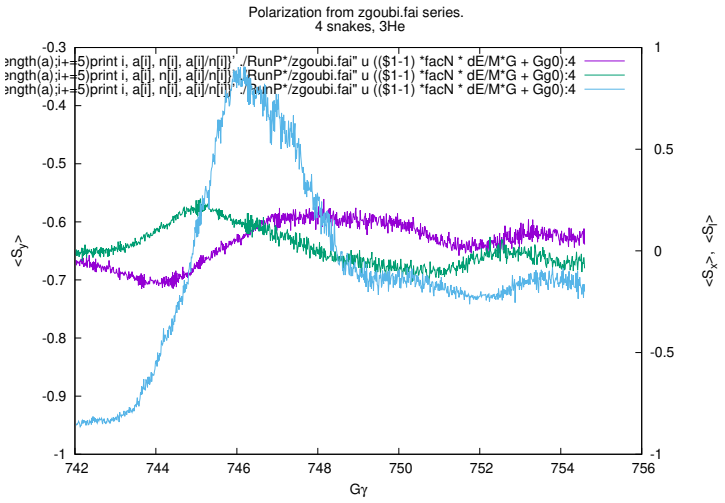

Figure 47: Turn-by-turn $\langle S_y \rangle$, $\langle S_l \rangle$ and $\langle S_x \rangle$ 500 particle averages across 717+ν_y, helion. $\hat{V} = 70\,\text{kV}$.

• snakes(axis angle) at
7(+22.5)-9(-22.5)-11(+22.5)-3(-22.5) o'clock
defect vertical orbit 0.6 mm rms
voltage 35kV

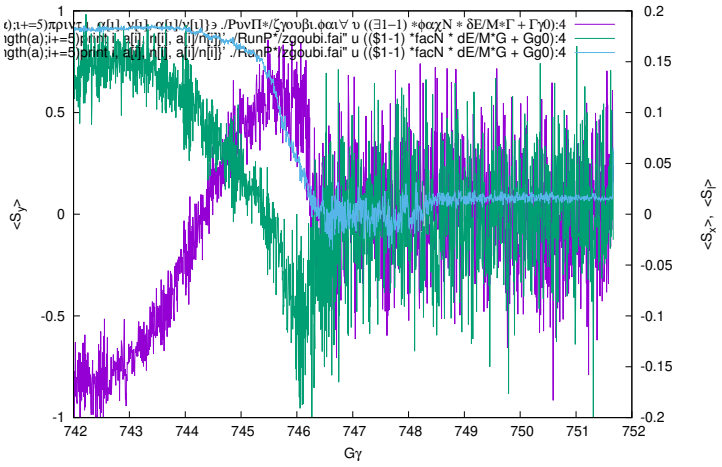

Figure 48: Turn-by-turn $\langle S_y \rangle$, $\langle S_l \rangle$ and $\langle S_x \rangle$ 100 particle averages across 717+ν_y, helion.

References

[1] M.Bai, P. Cameron, A. Luccio, H. Huang, V. Ptitsyn, T. Roser, S. Tepikian: SNAKE DEPOLARIZING RESONANCE STUDY IN RHIC. TUPAS086, Proceedings of PAC07, Albuquerque, New Mexico, USA.
https://accelconf.web.cern.ch/p07/PAPERS/TUPAS086.PDF

[2] F. Méot: Spin dynamics. In: Polarized Beam Dynamics and Instrumentation in Particle Accelerators. Springer, 2023.
https://link.springer.com/book/10.1007/978-3-031-16715-7

[3] Lee, S.Y: Spin Dynamics and Snakes in Synchrotrons. World Scientific (1997)